MASS SPLITTINGS OF HEAVY QUARK SPIN SYMMETRY PARTNERS OF $X(3872)$ IN QCD SUM RULES

A THESIS SUBMITTED TO
THE GRADUATE SCHOOL OF NATURAL AND APPLIED SCIENCES
OF
MIDDLE EAST TECHNICAL UNIVERSITY

BY

HANDE ÇETİN

IN PARTIAL FULFILLMENT OF THE REQUIREMENTS
FOR
THE DEGREE OF MASTER OF SCIENCE
IN
PHYSICS

SEPTEMBER 2021

Approval of the thesis:

MASS SPLITTINGS OF HEAVY QUARK SPIN SYMMETRY PARTNERS OF $X(3872)$ IN QCD SUM RULES

submitted by **HANDE ÇETİN** in partial fulfillment of the requirements for the degree of **Master of Science in Physics Department, Middle East Technical University** by,

Prof. Dr. Halil Kalıpçılar
Director, Graduate School of **Natural and Applied Sciences** _____

Prof. Dr. Seçkin Kürkçüoğlu
Head of Department, **Physics** _____

Prof. Dr. Altuğ Özpineci
Supervisor, **Physics, METU** _____

Examining Committee Members:

Prof. Dr. İsmail Turan
Physics, METU _____

Prof. Dr. Altuğ Özpineci
Physics, METU _____

Dr. Hüseyin Dağ
Physics, Bursa Technical University _____

Date:09.09.2021

I hereby declare that all information in this document has been obtained and presented in accordance with academic rules and ethical conduct. I also declare that, as required by these rules and conduct, I have fully cited and referenced all material and results that are not original to this work.

Name, Surname: Hande Çetin

Signature :

ABSTRACT

MASS SPLITTINGS OF HEAVY QUARK SPIN SYMMETRY PARTNERS OF $X(3872)$ IN QCD SUM RULES

Çetin, Hande
M.S., Department of Physics
Supervisor: Prof. Dr. Altuğ Özpineci

September 2021, 68 pages

The parameters of QCDSR such as the values of the condensates and the Borel mass are not well-established and hence increase the uncertainty of predictions up to 30%. In this study, mass splittings of the heavy quark spin symmetry partners of the exotic particle $X(3872)$ are studied from the tetraquark aspect. In order to accomplish the task, randomised sets of the parameters are generated to find the squared mass values of the partners, and the results are compared with the findings in the literature. Randomisation of the values is performed using Wolfram Mathematica 12.0.0 and the data is analysed in Python 3.7.3.

Keywords: X(3872), tetraquark, QCD, Sum Rule

ÖZ

KRD TOPLAM KURALLARI İLE $X(3872)$ AĞIR KUARK SPİN SİMETRİ EŞLERİNİN KÜTLE AYRIŞIMLARI

Çetin, Hande
Yüksek Lisans, Fizik Bölümü
Tez Yöneticisi: Prof. Dr. Altuğ Özpineci

Eylül 2021 , 68 sayfa

KRDTK'nin kondensat ve Borel kütlesi gibi değişkenlerinin tam değerleri üzerinde anlaşılmamıştır ve bu da sonuçtaki hata payını $\%30$'a kadar arttırabilmektedir. Bu çalışmada $X(3872)$ egzotik parçacığı ağır kuark spin simetri eşleri tetrakuark olarak incelenmiştir. Bunun için bahsi geçen değişkenlerin belirli aralıkları arasından rastgele seçilip takımlar oluşturulup söz konusu mezonların kütle kare değerleri elde edilmiştir. Değişken değerlerinin rastgele seçimleri Wolfram Mathematica 12.0.0, elde edilen verinin işlenmesi Python 3.7.3 ile gerçekleştirilmiştir.

Anahtar Kelimeler: X(3872), tetrakuark, KRD, Toplam Kuralları

To my future self to find some minor grammatical errors in couple years

ACKNOWLEDGMENTS

I would like to start with the acknowledgement of how grateful I am for my supervisor Altuğ Özpineci whose patience for my novice start on the subject I am indebted to and the person I have learned so much about the field from, Takhmasib Aliev. I would also like to thank İsmail Turan and Elif Cincioğlu for showing me the exciting nature of particle physics. I am also thankful for my family and friends for being there for me when needed. I would also like to acknowledge my growth both personally and as a prospective scientist supported by Emre Aşkan. Last, I would like to thank my pets Skadi and Bellatrix for being the light in some dark times in the years and the ones I have unfortunately lost along the way, Tarçın and Куся who are missed dearly.

TABLE OF CONTENTS

ABSTRACT v

ÖZ vi

ACKNOWLEDGMENTS viii

TABLE OF CONTENTS ix

LIST OF TABLES xi

LIST OF FIGURES xii

LIST OF ABBREVIATIONS xiv

CHAPTERS

1 INTRODUCTION 1

1.1 Method 1

1.2 Models 6

1.3 Thesis Structure 8

2 QCDSR 9

2.1 Introduction 9

2.2 Construction of the Sum Rule in SVZSR 10

2.2.1 Operator Product Expansion 10

2.2.2 Phenomenological Approach 18

2.2.3 Obtaining Mass 24

3 COMPUTATIONAL ANALYSIS 31

4 CONCLUSION 49

REFERENCES 53

A MATHEMATICAL EXPRESSIONS 61

A.1 Gamma Function Integral Identities 61

A.2 Heaviside Function Integral Representation 61

A.3 Borel Transformation 62

A.4 Polarisation Operator Identities 62

B LIST OF COEFFICIENTS 65

C LIST OF INTEGRAL IDENTITIES 67

LIST OF TABLES

TABLES

Table 1.1 Experiments on the discovery and the confirmation on $X(3872)$. . . 2

Table 3.1 Randomisation ranges for the corresponding variables with the control values 32

Table 4.1 Summary of squared mass comparison results. †: Upper bound is not set precisely. 49

Table B.1 Coefficients of Borel transformed integrals with their corresponding coefficients for their derivatives 66

LIST OF FIGURES

FIGURES

Figure 2.1 Contour over the complex plane t where the branch cut is shown darker. 20

Figure 3.1 Distribution of $m^2_{2^{++}}$ values from $\Pi^{(2)}$ 34

Figure 3.2 Highest peak distribution of $m^2_{2^{++}}$ values from $\Pi^{(2)}$ 34

Figure 3.3 Distribution of $m^2_{1^{++}}$ values from $\Pi^{(2)}$ 35

Figure 3.4 Highest peak distribution of $m^2_{1^{++}}$ values from $\Pi^{(2)}$ 35

Figure 3.5 Distribution of $m^2_{0^{++}}$ values from $\Pi^{(2)}$ 37

Figure 3.6 Highest peak distribution of $m^2_{0^{++}}$ values from $\Pi^{(2)}$ 37

Figure 3.7 Distribution of $m^2_{1^{++}}$ values from $\Pi^{(1)}$ 38

Figure 3.8 Highest peak distribution of $m^2_{1^{++}}$ values from $\Pi^{(1)}$ 38

Figure 3.9 Distribution of $m^2_{1^{-+}}$ values from $\Pi^{(1)}$ 40

Figure 3.10 Highest peak distribution of $m^2_{1^{-+}}$ values from $\Pi^{(1)}$ 40

Figure 3.11 Distribution of $m^2_{0^{++}}$ values from $\Pi^{(0)}$ 41

Figure 3.12 Highest peak distribution of $m^2_{0^{++}}$ values from $\Pi^{(0)}$ 41

Figure 3.13 Distribution of $m^2_{2^{++}} - m^2_{1^{++}}$ values from $\Pi^{(2)}$ 43

Figure 3.14 Highest peak distribution of $m^2_{2^{++}} - m^2_{1^{++}}$ values from $\Pi^{(2)}$ . . . 43

Figure 3.15 Distribution of $m^2_{0^{++}} - m^2_{1^{++}}$ values from $\Pi^{(2)}$ 45

Figure 3.16 Highest peak distribution of $m^2_{0^{++}} - m^2_{1^{++}}$ values from $\Pi^{(2)}$ . . . 45

Figure 3.17 Distribution of $m^2_{1^{-+}} - m^2_{1^{++}}$ values from $\Pi^{(1)}$ 47

Figure 3.18 Highest peak distribution of $m^2_{1^{-+}} - m^2_{1^{++}}$ values from $\Pi^{(1)}$ . . . 47

LIST OF ABBREVIATIONS

QCD	Quantum Chromodynamics
QCDSR	Quantum Chromodynamics Sum Rule
SVZ	Shifman-Vainshtein-Zakharov
SVZSR	Shifman-Vainshtein-Zakharov Sum Rules
OPE	Operator Product Expansion
KRD	Kuantum Renk Dinamiği
SM	Standard Model
LHCb	Large Hadron Collider Beauty (b) Experiment
SLAC	Stanford Linear Accelerator Center
CDF	Collider Detector at Fermilab
D∅	DZero experiment
BESIII	Beijing Spectrometer Experiment
QED	Quantum Electrodynamics

CHAPTER 1

INTRODUCTION

1.1 Method

Particles called hadrons interact via strong interaction and are made up of quarks and gluons. Properties of hadrons such as mass and quantum numbers help to establish the basis on which the assumptions about the existence of more particles can be made theoretically, and then the experiments can be performed on these expectations in order to determine the validity of the constructed theory. Thus, through the experiments, new particles are searched for in the theoretically established ranges. A particle is called an exotic particle if the experimental observation is not in full agreement with the expectations of the quark model in some aspects.

Such particles have been observed in many experiments including decays, collisions, and scatterings. These particles are referred to with their initially observed masses, and the property of their states if axial vector, X; vector state, Y; charged state, Z; which are on the charmonium spectrum [1]. One of the many important exotic particles is $X(3872)$ which is observed in $B^{\pm} \rightarrow K^{\pm}\pi^{+}\pi^{-}J/\psi$ process initially by Belle [2]. Also observed by *BABAR*, LHCb, CDF, (BESIII) D$\emptyset$, and BESIII in the given processes in Table1.1. The significance of $X(3872)$, also referred to as $\chi_{C1}(3872)$, among all exotic particles is that since its first discovery, $X(3872)$ is one of the particles whose properties are known the most. Furthermore, quark model expects a particle with charmonium content in this range, but the expected mass value and observed mass are off by 50 MeV [3].

Exotic particles have been studied with the methods of QCD in order to understand their behaviour and properties such as their quantum numbers. The ones that are

m (MeV)	J^{PC}	Process (produced in or decay mode)	Experiment
$3872.0 \pm 0.6 \pm 0.5$		$B^{\pm} \to K^{\pm}\pi^+\pi^- J/\psi$	Belle [2]
3871.2 ± 0.5		$B^+ \to X(3872)K^+$ $B^0 \to X(3872)K^0_s$ $X(3872) \to J/\psi\pi^+\pi^-$	Belle [4]
3873.4 ± 1.4		$B^- \to X(3872)K^-$ $X(3872) \to J/\psi K^-\pi^+\pi^-$	*BABAR* [5]
$3871.84 \pm 0.27 \pm 0.19$	$1^{++}/2^{-+}$	$B^+ \to X(3872)K^+ \to K^+(\pi^+\pi^- J/\psi)$ $B^0 \to X(3872)K^0 \to K^0(\pi^+\pi^- J/\psi)$	Belle [6]
$3871.3 \pm 0.7 \pm 0.4$		$X(3872) \to J/\psi\pi^+\pi^-$	CDF II [7]
$3871.61 \pm 0.16 \pm 0.19$		$X(3872) \to J/\psi\pi^+\pi^-$	CDF [8]
	$1^{++}/2^{-+}$	$X(3872) \to J/\psi\pi^+\pi^- \to (\mu^+\mu^-)\pi^+\pi^-$	CDF [9]
		$B^+ \to X(3872)K^+ \to K^+(\pi^+\pi^- J/\psi)$ $B^0 \to X(3872)K^0 \to K^0(\pi^+\pi^- J/\psi)$	*BABAR* [10]
3871.8 ± 6.1		$X(3872) \to J/\psi\pi^+\pi^- \to (\mu^+\mu^-)\pi^+\pi^-$	DØ [11]
		$X(3872) \to \gamma J/\psi$ $X(3872) \to J/\psi\pi^+\pi^-\pi^0$	Belle [12]
$3873.0^{+1.8}_{-1.6} \pm 1.3$	$1^+/2^-$	$B^{0,+} \to K^{0,+}J/\psi\pi^+\pi^-\pi^0$	*BABAR* [13]
$3875.4 \pm 0.7^{+1.2}_{-2.0}$		$B \to KD^0\bar{D}^0\pi^0$	Belle [14]
	$1^{++}/2^{++}$		Belle [15]
$3872.9^{+0.6+0.4}_{-0.4-0.5}$		$B \to X(3872)D^{*0}\bar{D}^0$	Belle [16]
$3875.1^{+0.7}_{-0.5} \pm 0.5$	$1^+/1^-$	$B \to \bar{D}^* D^* K$	*BABAR* [17]
		$B^+ \to K^+X(3872) \to J/\psi\gamma K^+$	*BABAR* [18]
		$B \to K^{\pm,0,*}X(3872) \to K^{\pm,0,*}{}^{J/\psi}_{\psi(2S)}\gamma$	*BABAR* [19]
3873.4 ± 3.4 3869.5 ± 3.4		$B^+ \to K^+X(3872) \to K^+J/\psi\gamma$ $B^+ \to K^+X(3872) \to K^+\psi(2S)\gamma$	LHCb [20]
$3871.9 \pm 0.7 \pm 0.2$		$e^+e^- \to X(3872)\gamma$	BESIII [21]
$3871.95 \pm 0.48 \pm 0.12$		$pp \to X(3872) + ...$	LHCb [22]
	1^{++}	$B^+ \to X(3872)K^+ \to K^+(\pi^+\pi^- J/\psi) \to K^+\pi^+\pi^-(\mu^+\mu^-)$	LHCb [23]

Table 1.1: Experiments on the discovery and the confirmation on $X(3872)$.

observed in the strong interactions are tested using the methods of QCD which is the study of strong interactions mediated by the gluons and quarks as the constituents of the interactions [24].

The foundation of QCD started with the categorisation of the known baryons using the mindset of group theory into octet (SU(2)), and decuplet (SU(3)) by Gell-Mann, Ne'eman and Heisenberg [25–27]. After that, quarks were defined in the theory as the constituents of the strong interaction by Gellmann [28] and Zweig [29]. Following that, Björken's and Bander's previous predictions on the scaling behaviour of the

cross section [30] stating the value of cross section depended mainly on the mass of the virtual photon and the energy transfer at low energies, but at large energies, the value depended mostly on the ratio of the virtual photon mass and the energy transfer were observed at SLAC on the deep-inelastic scattering of electron and atomic nuclei experiments [31]. Next, the colour charge was introduced with SU(3) symmetry so as to explain the behaviour of the baryons such as Ω^- of not obeying Pauli's principle, but rather obeying a "para-statistics of rank three" as Harald Fritzch [32], one of the pioneers of the theory, expresses. Lastly, the mediator of the interaction, gauge bosons were identified as the gluons [33]. Representing dynamics of the strong interaction, Lagrangian of the QCD is described as

$$\mathcal{L}_{QCD} = \overline{\psi}_i \left(i \, \gamma^\mu \partial_\mu - m \right) \psi_i - g_S \, \overline{\psi}_i \lambda^a_{ij} \psi_j \gamma^\mu A^a_\mu - \frac{1}{4} G^{a\mu\nu} G^a_{\mu\nu} \tag{1.1}$$

where i and j represent quark flavours which can be up (u), down (d), charm (c), strange (s), top (t), and bottom or beauty (b) with

$$G^a_{\mu\nu} = \partial_\mu A^a_\nu - \partial_\nu A^a_\mu - g_S \, f^{abc} A^b_\mu A^c_\nu \tag{1.2}$$

where ψ_i represents the quark field, a, b, and c are the colour index which can be red, green, and blue of the tensors such as the field strength tensor $G^a_{\mu\nu}$ or A^a_μ which is the gluon field of colour, $g_S = \sqrt{4\pi\alpha_S}$ is the strong coupling constant, f^{abc} is the structure constant of the SU(3) colour group, and λ are the Gell-Mann matrices that are the generators of the SU(3) colour group. The first term is the free Dirac Lagrangian of the quarks and leads to quark propagators while the second term represents the quark-gluon interactions. The last term is the gluon field Lagrangian and produces the gluon propagator similarly to the photon propagator obtained from QED Lagrangian. In addition to the gluon propagator, this term also encapsulates the triple and quadruple gluon vertices which is the reason for asymptotic freedom, gluon self-interactions.

Since the first emergence of QCD, many methods were developed to investigate the properties of its spectrum, i.e. the hadrons. These methods include Sum Rules which had prior applications before the foundation of QCD explaining the strong interactions as well. Prior sum rules such as the Drell-Hearn sum rule and the Adler-Weisberger had been established to explain hadrons using the tools that are continued

to be employed in QCDSR. The tools used are the dispersion relations for Compton Scattering, the optical theorem in order to associate the total cross sections to the scattering amplitudes, and a low energy theorem to regulate the scattering amplitudes at zero energy [34]. These prior sum rules have had applications apart from QCD such as the perturbation theory in which Drell-Hearn was tested with the theories constructing the basis of QED or the phenomenological study of the deep inelastic scattering of polarised particles of leptons onto polarised protons. Adler-Weisberger Sum Rule was used to relate the axial coupling constant g_A from β decay to the integrals of pion-nucleon total cross sections using the same tools with additional approximation methods. The sum rule was tested with the current up-to-date methods and tools and the resulting one loop level calculations yield almost the same result with few minor constants. Another prior sum rule method is the Weinberg Sum Rules which have present applications, and further, predictions on the strong interactions. One of the current applications can be examined on a correlation function below that is notably responsive to the chiral symmetry breaking.

$$\Pi_{LR}^{\mu\nu} = 2\,i \int d^4x\, e^{iqx} \langle 0|\, T\left\{L^{\mu}(x) R^{\nu\dagger}(0)\right\} |0\rangle \tag{1.3}$$

where the currents are

$$L^{\mu}(x) = \overline{d}(x)\gamma^{\mu}\frac{1}{2}\left(1-\gamma_5\right)u(x) \qquad R^{\mu}(x) = \overline{d}(x)\gamma^{\mu}\frac{1}{2}\left(1+\gamma_5\right)u(x). \tag{1.4}$$

The correlation function in Equation 1.3 corresponds to the difference of a vector current correlation function and an axial vector current correlation function as

$$\begin{aligned} \int_0^{\infty} dt\ \mathrm{Im}\left\{\Pi_{LR}(t)\right\} &\equiv \int_0^{\infty} dt\ \mathrm{Im}\left\{\Pi_V(t) - \Pi_A(t)\right\} \\ \int_0^{\infty} dt\, t\ \mathrm{Im}\left\{\Pi_{LR}(t)\right\} &\equiv \int_0^{\infty} dt\, t\ \mathrm{Im}\left\{\Pi_V(t) - \Pi_A(t)\right\} \end{aligned} \tag{1.5}$$

where Π_V represents the correlation function corresponding to a vector current and Π_A represents the correlation function of an axial vector current. These sum rules

obey the unsubtracted dispersion relation

$$\Pi_{LR}(Q^2) = \int_0^\infty \frac{dt}{t+Q^2} \operatorname{Im}\left\{\Pi_{LR}(t)\right\}. \tag{1.6}$$

The sum rules on Equation 1.5 correspond to the constraints

$$\begin{aligned} \lim_{Q^2\to\infty} Q^2\ \Pi(Q^2) &\to 0 \\ \lim_{Q^2\to\infty} Q^4\ \Pi(Q^2) &\to 0. \end{aligned} \tag{1.7}$$

Above constraints (Equations 1.7) are now accepted as the properties of quantum chromodynamics. Of these sum rules Weinberg proposed 1.5, the first is still valid for the finite light quark masses [34]. After QCD was established as the theory of strong interactions, many other methods emerged. One of these methods is the SVZ Sum Rules that is constructed by Shifman, Vainshtein, and Zakharov [35, 36] which will also be adopted in this study. This method has been one of the most commonly used analytical methods to explain the exotic particles as it explains essential aspects of the many exotic particles [37–39]. The advantages of using this method can be acknowledged while examining the hadronic particles in the bottomonium and charmonium spectra as it has been fruitful to clarify many of the details. Furthermore, the experimental values are observed to match the expected values obtained from the SVZSR method theoretically. Making use of the asymptotic freedom, quark and gluon interactions are separated into perturbative and nonperturbative parts whose former is mostly divergent hence examined separately and latter is used to proceed into the sum rule.

As with any theory, there are also shortcomings of this method such as the large margin of uncertainty. The origin of uncertainty depends mostly on duality, the values of condensates not being established, and the choice of continuum threshold not being agreed upon. Also, the Borel transformation introducing another unknown parameter whose window of values and choice varies the result to a degree. Likewise, the fact that the exclusion of higher dimension terms in the OPE as analytical and computational sums need to truncate the infinite sums at some point brings the error margins to an extension. In addition, perturbative terms have finite accuracy due to alterations

in the coupling constant which affects the results of the value of the decay constant when collected in the continuum part of the sum rule [1]. There is also the unheeded possibility of direct instanton contributions [39, 40].

In this study, the purpose is to calculate the uncertainties in the predictions of the masses more reliable by scanning the parameter space spanned by the variables s_0 threshold, M^2 Borel parameter, both condensates $\langle\bar{q}q\rangle$ quark and $\left\langle G^a_{\mu\nu}G^{a\mu\nu}\right\rangle$ gluon, and m_0^2 whose margins are taken from [40].

1.2 Models

Many models were suggested after the discovery [2] of the exotic particle $X(3872)$ [3, 41–53] as it was the first particle in the charmonium spectrum discovered that did not fit into the expectations of the potential quark model. These models propose $X(3872)$ to be either tetraquark, meson molecule, hybrid charmonium or hadro-charmonium. In the meson molecule approach, the four quarks combine in such a manner that creates the particle as the bound state of two mesons [38, 44, 46, 48]. Next, hybrid charmonium approach suggests a charmonium structure presence along with a glueball or a gluon field [3, 42, 44]. The hadro-charmonium model suggests that the particle is in the form of a molecule structure where one of the mesons is a charmonium [1, 54]. Last, in the tetraquark model, the structure consists of four quarks in the form of two quark-antiquark couples or a diquark-antidiquark structure [53, 55–57].

In addition to the proposed structures, one needs to consider the spin-flavour symmetry as it results in special properties for the hadrons that involve heavy quarks. In the limit of $m_Q \to \infty$, strong interactions have conserved attributes of the heavy quark spin and the total angular momentum j of the light degrees of freedom. Furthermore, the dynamics are independent of the spin and mass of the heavy quark due to the heavy quark symmetry. Therefore, the hadron at hand can be represented with the quantum numbers such as spin, parity, and flavour of the light degrees of freedom which results in the degeneracy of hadronic states [58]. In the case of a ground state particle containing a heavy quark as proposed here for $X(3872)$, the degenerate states

will be $J = 0$ for the pseudo-scalar, $J = 1^-$ for the vector, $J = 1^+$ for the axial vector, and $J = 2$ for when each of the values of the heavy quark spin and the light quark spin values sums up to 1, in total 2. Among these degenerate states, the ones that are mostly discussed for $X(3872)$ are 2^{++}, 1^{++}, 1^{-+}, 0^{++}, 0^{-+} [14, 59–61].

All the proposed structures are involved in different dynamics. First, charmonium states have gluon exchange dominance at short-range interactions and confining long-range non-perturbative interactions which require a linear potential like Cornell potential. Second, for the hybrid charmonium, there is also the excitations of the gluon field which is referred to as flux tubes. Among all the models proposed, meson molecule and tetraquark structures are the primarily argued ones. Mass obtained for $X(3872)$ from QCDSR does not distinguish the structure configuration as tetraquark or meson molecule as the currents are related only via the transformation below

$$\begin{aligned} j_{\mu\nu}^{tq} &= \left(\bar{Q}^a \, \Gamma_\mu \, Q^a\right) \left(\bar{q}^b \, \Gamma_\nu \, q^b\right) \\ j_\mu^{mm} &= \frac{1}{\sqrt{2}} \left[\left(\bar{q}^a \, \gamma_5 \, Q^a \bar{Q}^b \, \gamma_\mu \, q^b\right) - \left(\bar{q}^a \, \gamma_\mu \, Q^a \bar{Q}^b \, \gamma_5 \, q^b\right)\right] \\ j_\mu^{di} &= \frac{i\epsilon_{abc}\epsilon_{dec}}{\sqrt{2}} \left[\left(q_a^T \, C\gamma_5 \, Q_b\right) \left(\bar{q}_d \, \gamma_\mu C \, \bar{Q}_b^T\right) + \left(q_a^T \, C\gamma_\mu \, Q_b\right) \left(\bar{q}_d \, \gamma_5 C \, \bar{Q}_b^T\right)\right] \end{aligned} \tag{1.8}$$

where C is the charge conjugation matrix and Γ_μ are the Dirac matrices [1, 62, 63]. On one hand, in the molecule structure, the internal interaction dynamics occurs via meson exchange. On the other hand, in the tetraquark structure, there is a possibility of an additional interaction dynamic involving a diquark-antidiquark interaction which is not yet well-established and is used in the form j_μ^{di} above [1, 62, 64].

In order to describe exotic particles within the SVZ QCDSR approach, the interpolating currents are joined together with an additional pair of quark-antiquark pair and these four quarks give rise to a higher number of permutations for the Feynman diagrams and these diagrams are referred to as "petal" forms as shown in Figure 3 of [1] which shows the OPE for the three-point function written in terms of exotic interpolating current. Also, colour connected diagrams, which involve a gluon exchange, suggest a tetraquark structure rather than a meson molecule as two petals cannot be considered as two separate mesons to form the molecule configuration [1, 65–68]. Therefore, throughout this study, the exotic particle $X(3872)$ will be examined as a tetraquark where the structure involves charm as the heavy quarks and the J^{PC} values

of the partners will be studied as 2^{++}, 1^{++}, 1^{-+}, and 0^{++}.

In this study, the aim is to study the mass splitting of the partners of $X(3872)$ particle with the QCDSR approach described in [39] in order to find out which one of its partners is more stable with respect to the variations in parameters that are Borel mass, condensates, continuum threshold (s_0) and more compatible with the experimental results and conclude if the structure being tetraquark is favourable to meson molecule model as the tetraquark structure masses are below threshold due to the lack of binding energy between mesons in the meson molecule [69].

The two point Green function will be constructed using the currents given in [70]. It will then be operated on to yield the mass term as in Chapter 2 for each of the quantum numbers of the partners of $X(3872)$.

1.3 Thesis Structure

The thesis consists of four chapters in total in which the next one (Chapter 2), the analytical method is used to compute the form of the squared mass of $X(3872)$ particle in detail. Then, in Chapter 3, the computational analysis of the mass splittings will be examined. Last, in Chapter 4, the results obtained will be discussed and the conclusion will be given.

CHAPTER 2

QCDSR

2.1 Introduction

In this study, strong interactions are to be examined using the SVZ sum rule methods, i.e. QCDSR. Construction of a sum rule requires examining a two-point Green function in two different approaches and equating later to find the desired information such as coupling constant, magnetic moment, and mass. In this work, the procedure to be followed is adopted from [39] and the values to be extracted to be closely examined from the sum rule are of the masses.

The sum rule method to be used throughout this study is the SVZSR that employs the use of Wilson's OPE in order to explain the properties of the particle at hand. In this method, the two-point Green function that is the correlation function is defined in the currents and extracted as coefficients referred to as Wilson's coefficients of the operators in the sum corresponding to the time-ordered product. The time-ordered product will then be taken in a vacuum bra-ket expression and these operators in the sum will produce condensates which are fluctuations in the fields constituting the vacuum of the theory. The expansion of the terms for the time-ordered product can be represented as follows

$$T\{j_{\alpha\beta}(x)j^{\dagger}_{\gamma\delta}(0)\} = \sum_{n} c_n(x,\mu)\,\mathcal{O}(0,\mu) \tag{2.1}$$

for $x \ll \Lambda^{-1}_{QCD}$. The operators are condensates that are normal ordered. The orders of these are the identity $\mathbb{1}$, light quark mass $m_q(\mathbb{1})$, quark condensate $\langle\overline{q}q\rangle$, gluon condensate $\left\langle G^{a}_{\mu\nu}G^{a\mu\nu}\right\rangle$ and mixed condensates such as $m_q\langle\overline{q}q\rangle$ in the higher orders of the expansion. The analytical computation here will be taken until $\langle\overline{q}q\rangle$ order.

2.2 Construction of the Sum Rule in SVZSR

The first step in the establishing of the sum rule is to construct a correlation function using the interpolating currents as

$$\Pi_{\alpha\beta;\delta\gamma} = i \int d^4x \; e^{ikx} \langle 0| \, T\{j_{\alpha\beta}(x) j^{\dagger}_{\gamma\delta}(0)\} \, |0\rangle \tag{2.2}$$

and examining the correlation function in the Equation 2.2 in two ways by making use of the quark hadron duality. Later, both sides will be equated and Borel transformation will be performed on both so as to obtain the desired information, in this study, mass.

2.2.1 Operator Product Expansion

The first part starts with the expansion of the currents in terms of the quark fields and Dirac matrices (Γ_i), which are $\mathbb{1}$, γ^μ, $\sigma^{\mu\nu}$, $\gamma^\mu\gamma^5$, and γ^5, which are of the form $\langle \bar{q}\gamma^\mu q\rangle$ for vector current, $\langle \bar{q}\gamma^\mu\gamma^5 q\rangle$ for axial-vector current, $G^{a\mu\nu}G^a_{\mu\nu}$ for gluon fields or $\bar{q}\Gamma q\bar{q}\Gamma q$ for the composite operator which also includes the vector current expression inside the bra-ket. Here, the current is in the form of a composite operator of two vector currents as follows.

$$j^q_{\alpha\beta} = \overline{Q^a}(x)\gamma_\alpha Q^b(x) \, \overline{q^b}(x)\gamma_\beta q^a(x) \tag{2.3}$$

with components Q as the heavy quark which is the charm quark in this study, and q as the light quark that is either *up* (u) or *down* (d) quark. Here, a and b are the colour indices. Substituting the current in Equation 2.3 into the correlation function results in

$$\begin{aligned}\Pi_{\alpha\beta;\delta\gamma} = i \int d^4x \; e^{ikx} \langle 0| \, T\{&\overline{Q^a}(x)\gamma_\alpha Q^b(x) \, \overline{q^b}(x)\gamma_\beta q^a(x) \\ &\overline{Q^d}(0)\gamma_\gamma Q^e(0) \, \overline{q^e}(0)\gamma_\delta q^d(0)\} \, |0\rangle \, .\end{aligned} \tag{2.4}$$

At this point, the time-ordered product is converted into a normal ordered product using Wick's theorem.

Possible contractions are

$$\begin{aligned}
&\overline{q^b}(x)\, q^d(0)\\
&q^a(x)\, \overline{q^e}(0)\\
&\overline{Q^a}(x)\, Q^e(0)\\
&Q^b(x)\, \overline{Q^d}(0)
\end{aligned} \tag{2.5}$$

which have many number of combinations. Nonetheless, only the first few condensate terms will be calculated here to show the details of the work in this study that are $\mathbb{1}$, m_q, and $\langle\bar{q}q\rangle$. These terms will only have contributions from the fully contracted term or the terms with three contraction of those two are the heavy quark fields. Considering the fully contracted combination,

$$\Pi_{\alpha\beta;\delta\gamma} = i\int d^4x\, e^{ikx}\, \langle 0|:\overline{Q^a}\gamma_\alpha Q^b\overline{q^b}\gamma_\beta q^a\overline{Q^d}\gamma_\delta Q^e\overline{q^e}\gamma_\gamma q^d:|0\rangle\,. \tag{2.6}$$

Inside of the normal ordered product can be collected into their corresponding propagators

$$\left[\overline{Q^a}\right]_\mu(\gamma_\alpha)_{\mu\nu}\left[Q^b\right]_\nu\left[\overline{q^b}\right]_\eta(\gamma_\beta)_{\eta\theta}\left[q^a\right]_\theta\left[\overline{Q^d}\right]_\kappa(\gamma_\delta)_{\kappa\lambda}\left[\overline{Q^e}\right]_\lambda\left[\overline{q^e}\right]_\sigma(\gamma_\gamma)_{\sigma\rho}[q^d]_\rho.$$

$$\begin{aligned}
Q^e(0)_\lambda\,\overline{Q^a}(x)_\mu &= i\,S^Q_{\lambda\mu}(-x)\delta^{ea}, \quad & q^a(x)_\theta\,\overline{q^e}(0)_\sigma &= i\,S^q_{\theta\sigma}(x)\delta^{ae}\\
Q^b(x)_\nu\,\overline{Q^d}(0)_\kappa &= i\,S^Q_{\nu\kappa}(x)\delta^{bd}, & q^d(0)_\rho\,\overline{q^b}(x)_\eta &= i\,S^q_{\rho\eta}(-x)\delta^{db}.
\end{aligned} \tag{2.7}$$

After this, the propagators are substituted in the following form as given in [71]; later, the traces are constructed.

$$\begin{aligned}
S_q(x) &= \left[\frac{i\not{x}}{2\pi^2x^4} - \frac{m_q}{4\pi^2x^2}\right]\\
S_Q(x) &= \left[\frac{m_Q^2}{4\pi^2}\frac{K_1(m_Q\sqrt{-x^2})}{\sqrt{-x^2}} - i\frac{m_Q^2\not{x}}{4\pi^2x^2}K_2(m_Q\sqrt{-x^2})\right]
\end{aligned} \tag{2.8}$$

$$K_n(m_Q\sqrt{-x^2}) = \frac{(m_Q)^n}{(-x^2)^{n/2}\,2^{n+1}}\int_0^\infty dt\; t^{(-n-1)}\,\exp\left[-\frac{m_Q^2}{4t} + tx^2\right] \tag{2.9}$$

where K_n are the modified Bessel functions of the second kind in the form of Equation 2.9. Substituting these yields the perturbative contributions of the correlation function into

$$\Pi^4_{\alpha\beta;\delta\gamma} = i \int d^4x \; e^{ikx} \delta^{ae}\delta^{bd}\delta^{ea}\delta^{db} \left[S^Q_{\lambda\mu}(-x)(\gamma_\alpha)_{\mu\nu} S^Q_{\nu\kappa}(x)(\gamma_\delta)_{\kappa\lambda}\right] \left[S^q_{\theta\sigma}(x)(\gamma_\gamma)_{\sigma\rho} S^q_{\rho\eta}(-x)(\gamma_\beta)_{\eta\theta}\right] \tag{2.10}$$

where the superscript 4 on $\Pi^4_{\alpha\beta;\delta\gamma}$ indicates the number of contractions.

As $\delta^{ae}\delta^{ea} = N_c$, and each parentheses above correspond to a trace, and using the propagators in the form of Equation 2.8, and the identity

$$\text{Tr}\left[\gamma_\mu\gamma_\gamma\gamma_\nu\gamma_\beta\right] = 4\left[g_{\mu\gamma}g_{\nu\beta} - g_{\mu\nu}g_{\gamma\beta} + g_{\mu\beta}g_{\gamma\nu}\right], \tag{2.11}$$

and abbreviating $K_n(m_{\bar{Q}}\sqrt{-x^2}) = K_n(m_Q\sqrt{-x^2})$ as K_n^- since $m_Q = m_{\overline{Q}}$.

$$\begin{aligned}
\text{Tr}\left[S^Q(-x)\,\gamma_\alpha\, S^Q(x)\gamma_\delta\right] &= \text{Tr}\left[\left[\frac{m_Q^2}{4\pi^2}\frac{K_1(m_Q\sqrt{-x^2})}{\sqrt{-x^2}} + i\frac{m_Q^2 \not{x}}{4\pi^2 x^2}K_2(m_Q\sqrt{-x^2})\right]\gamma_\alpha \right. \\
&\qquad \left.\left[\frac{m_Q^2}{4\pi^2}\frac{K_1(m_Q\sqrt{-x^2})}{\sqrt{-x^2}} - i\frac{m_Q^2 \not{x}}{4\pi^2 x^2}K_2(m_Q\sqrt{-x^2})\right]\gamma_\delta\right] \\
&= \left(\frac{m_Q}{2\pi}\right)^4 \left[\frac{8K_2^{2-}}{x^4}x_\alpha x_\delta - \frac{4}{x^2}(K_1^{2-} + K_2^{2-})g_{\alpha\delta}\right]
\end{aligned} \tag{2.12}$$

$$\begin{aligned}
\text{Tr}\left[S^q(x)\,\gamma_\gamma\, S^q(-x)\gamma_\beta\right] &= \text{Tr}\left[\left[\frac{i\not{x}}{2\pi^2x^4} + \frac{m_q}{4\pi^2x^2}\right]\gamma_\gamma\left[\frac{i\not{x}}{2\pi^2x^4} - \frac{m_q}{4\pi^2x^2}\right]\gamma_\beta\right] \\
&= \left[\frac{-4 + x^2m_q^2}{4x^6\pi^4}g_{\beta\gamma} + \frac{2}{\pi^4x^8}x_\beta x_\gamma\right]
\end{aligned} \tag{2.13}$$

both can be collected as

$$\begin{aligned}
\Pi^4_{\alpha\beta;\delta\gamma} = \int d^4x\, N_c^2\, e^{ikx}\left(\frac{m_Q}{2\pi}\right)^4 &\left[\frac{-4 + x^2m_q^2}{4x^6\pi^4}g_{\beta\gamma} + \frac{2}{\pi^4x^8}x_\beta x_\gamma\right] \\
&\left[\frac{8K_2^{2-}}{x^4}x_\alpha x_\delta - \frac{4}{x^2}(K_1^{2-} + K_2^{2-})g_{\alpha\delta}\right].
\end{aligned} \tag{2.14}$$

The next term in the OPE will be obtained from the two terms which have triple

contractions as below.

$$\Pi^{3.1}_{\alpha\beta;\delta\gamma} = i \int d^4x\, e^{ikx} \langle 0| : \overline{Q^a}\gamma_\alpha Q^b \overline{q}^b \gamma_\beta q^a \overline{Q^d} \gamma_\delta \overline{Q^e} \overline{q}^e \gamma_\gamma q^d : |0\rangle \tag{2.15}$$

$$\Pi_{\alpha\beta;\delta\gamma} = i \int d^4x\, e^{ikx} \langle 0| : \overline{Q^a}\gamma_\alpha Q^b \overline{q}^b \gamma_\beta q^a \overline{Q^d} \gamma_\delta Q^e \overline{q}^e \gamma_\gamma q^d : |0\rangle\,. \tag{2.16}$$

where the superscripts 3.1 and 3.2 represent the number of contractions and the order of the correlation functions. When the same operations are performed on the above terms with three contractions,

$$\begin{aligned}\Pi^{3.1}_{\alpha\beta;\delta\gamma} = \int e^{ikx} N_c\, \delta^{bd}\, \mathrm{Tr}\left[S^Q(-x)\gamma_\alpha S^Q(x)\gamma_\delta\right] \\ \langle 0| : \left[\overline{q^b}(x)_\eta (\gamma_\beta)_{\eta\theta} S^q_{\theta\delta}(x) (\gamma_\gamma)_{\delta\rho} q^d(0)_\rho\right] : |0\rangle\,.\end{aligned} \tag{2.17}$$

The trace of the heavy quark propagators will be the same as in fully contracted Π^4.

$$\begin{aligned}\Pi^{3.1}_{\alpha\beta;\delta\gamma} = \int e^{ikx} N_c\, \delta^{bd}\, \left(\frac{m_Q}{2\pi}\right)^4 \left[\frac{8K_2^{2-}}{x^4} x_\alpha x_\delta - \frac{4}{x^2}\left(K_1^{2-} + K_2^{2-}\right) g_{\alpha\delta}\right] \\ \langle 0| : \left[\overline{q^b}(x)\gamma_\beta S^q(x)\gamma_\gamma q^d(0)\right] : |0\rangle\end{aligned} \tag{2.18}$$

Taylor expanding the light quark field as

$$\overline{q^b}(x) = \overline{q^b}(0) + x^\nu \left(\partial_\nu\, \overline{q^b}(0)\right) \tag{2.19}$$

the bracket term can be reorganised as

$$[\gamma_\beta S^q(x)\gamma_\gamma]_{\eta\rho} \left\{\langle 0| : \overline{q^b}(0)_\eta q^d(0)_\rho : |0\rangle + \langle 0| : \left(x^\nu\, \partial_\nu\, \overline{q}^b(0)\right)_\eta q^d(0)_\rho : |0\rangle\right\} \tag{2.20}$$

for which one can use the following equations with δ^{bd} allowing to match the same coloured fields and $\delta^{\eta\rho}$ granting the yield of trace.

$$\begin{aligned}\left[\langle 0| : \overline{q^b}(0)_\eta q^d(0)_\rho : |0\rangle = A\, \delta^{bd}\delta_{\eta\rho}\right]\delta_{bd}\, \delta^{\eta\rho} \Rightarrow A = \frac{1}{4N_c}\langle\bar{q}q\rangle \\ \Rightarrow \langle 0| : \overline{q^b}(0)_\eta q^d(0)_\rho : |0\rangle = \frac{1}{4N_c}\langle\bar{q}q\rangle\, \delta^{bd}\delta_{\eta\rho}\end{aligned} \tag{2.21}$$

With the use of the free Lagrangian of QCD, the second term in Equation 2.20 will be constructed as

$$x^{\nu}\left[\langle 0|:\left(\partial_{\nu}\,\bar{q}^{b}(0)\right)_{\eta}q^{d}(0)_{\rho}:|0\rangle=B\,(\gamma_{\nu})_{\eta\rho}\,\delta^{bd}\right](\gamma^{\nu})_{\rho\eta}\,\delta_{bd}. \tag{2.22}$$

For the left hand side of the equation, selection of the Fock-Schwinger gauge in which $x^{\mu}A_{\mu}=0$ grants $x^{\mu}\partial_{\mu}=x^{\mu}D_{\mu}$ where $D_{\mu}=\partial_{\mu}-i\,q\,A_{\mu}$ which is the covariant derivative. Therefore the equation can be simplified as

$$\begin{aligned}&\text{l.h.s.}=x^{\nu}\,\langle 0|:(\overline{q}(0)\overleftarrow{\not{D}})_{\eta}q(0)_{\rho}:|0\rangle=i\,m_{q}\,x^{\nu}\,\langle 0|:\overline{q}(0)_{\eta}q(0)_{\rho}:|0\rangle\\&\text{r.h.s.}=N_{c}\,B\,\text{Tr}(\gamma_{\nu}^{2})=N_{c}\,B\,4\text{Tr}(\mathbb{1})=16N_{c}\,B\end{aligned} \tag{2.23}$$

which yields

$$B=\frac{i\,m_{q}}{16\,N_{c}}\,\langle\bar{q}q\rangle\Rightarrow x^{\nu}\,\langle 0|:\left(\partial_{\nu}\overline{q}^{b}(0)\right)_{\eta}q^{d}(0)_{\rho}:|0\rangle=\frac{i\,m_{q}\not{x}}{16\,N_{c}}\,\langle\bar{q}q\rangle\,. \tag{2.24}$$

Collecting together the terms in the Equation 2.20 will bring a trace

$$[\gamma_{\beta}S^{q}(x)\gamma_{\gamma}]_{\eta\rho}\left(\frac{1}{4N_{c}}\,\langle\bar{q}q\rangle+\frac{i\,m_{q}\not{x}}{16\,N_{c}}\,\langle\bar{q}q\rangle\right)_{\rho\eta}=\frac{-m_{q}}{8\pi^{2}x^{4}N_{c}}\left[2x_{\beta}x_{\gamma}+x^{2}g_{\beta\gamma}\right]\langle\bar{q}q\rangle\,. \tag{2.25}$$

Gathering all the terms together, one obtains

$$\begin{aligned}\Pi^{3.1}_{\alpha\beta;\delta\gamma}=N_{c}\int d^{4}x\,e^{ikx}\left(\frac{m_{Q}}{2\pi}\right)^{4}\left(\frac{-m_{q}}{8\pi^{2}x^{4}}\right)\\\left\{\frac{8K_{2}^{2-}}{x^{4}}x_{\alpha}x_{\delta}-\frac{4}{x^{2}}(K_{1}^{2-}+K_{2}^{2-})g_{\alpha\delta}\right\}\left[2x_{\beta}x_{\gamma}+x^{2}g_{\beta\gamma}\right]\langle\bar{q}q\rangle\,.\end{aligned} \tag{2.26}$$

When the procedure followed for $\Pi^{3.1}$ is repeated for the Equation 2.16, the resulting integral is

$$\begin{aligned}\Pi^{3.2}_{\alpha\beta;\delta\gamma}=N_{c}\int d^{4}x\,e^{ikx}\left(\frac{m_{Q}}{2\pi}\right)^{4}\left(\frac{m_{q}}{4\pi^{2}x^{4}}\right)\\\left\{\frac{8K_{2}^{2-}}{x^{4}}x_{\alpha}x_{\delta}-\frac{4}{x^{2}}(K_{1}^{2-}+K_{2}^{2-})g_{\alpha\delta}\right\}\left[x_{\beta}x_{\gamma}-3x^{2}g_{\beta\gamma}\right]\langle\bar{q}q\rangle\,.\end{aligned} \tag{2.27}$$

Here, the projection operators given in the [70] will be employed that are

$$\begin{aligned}
\mathcal{P}^{0}_{\mu\nu;\bar{\mu}\bar{\nu}} &= \frac{1}{4} g_{\mu\nu} g_{\bar{\mu}\bar{\nu}} \\
\mathcal{P}^{1}_{\mu\nu;\bar{\mu}\bar{\nu}} &= \frac{1}{2} \left(g_{\mu\bar{\mu}} g_{\nu\bar{\nu}} - g_{\mu\bar{\nu}} g_{\nu\bar{\mu}} \right) \\
\mathcal{P}^{2}_{\mu\nu;\bar{\mu}\bar{\nu}} &= \frac{1}{2} \left(g_{\mu\bar{\mu}} g_{\nu\bar{\nu}} + g_{\mu\bar{\nu}} g_{\nu\bar{\mu}} - \frac{1}{2} g_{\mu\nu} g_{\bar{\mu}\bar{\nu}} \right)
\end{aligned} \tag{2.28}$$

which are to project on the current $j^{\mu\nu}$ into its irreducible presentations under the Lorentz group

$$\begin{aligned}
j^{0}_{\mu\nu} &= \mathcal{P}^{0}_{\mu\nu;\bar{\mu}\bar{\nu}} j^{\bar{\mu}\bar{\nu}} \\
j^{1}_{\mu\nu} &= \mathcal{P}^{1}_{\mu\nu;\bar{\mu}\bar{\nu}} j^{\bar{\mu}\bar{\nu}} \\
j^{2}_{\mu\nu} &= \mathcal{P}^{2}_{\mu\nu;\bar{\mu}\bar{\nu}} j^{\bar{\mu}\bar{\nu}} \\
j_{\mu\nu} &= j^{0}_{\mu\nu} + j^{1}_{\mu\nu} + j^{2}_{\mu\nu}
\end{aligned} \tag{2.29}$$

where 0, 1, 2 are the indicators at which the spin of the particle coupling to the corresponding current can take its maximum value.

Using the projection operators on Equation 2.28, $\Pi^{3.1}_{\alpha\beta;\delta\gamma}$, $\Pi^{3.2}_{\alpha\beta;\delta\gamma}$, and $\Pi^{4}_{\alpha\beta;\delta\gamma}$ contribu-

tions can be shown as

$$
\begin{aligned}
\Pi^{(0)3.1} &= \int d^4x\, e^{ikx} \left[\frac{m_Q^4\, m_q\, N_c}{64\pi^6 x^4}\right] (33K_1^{2-} - 8K_2^{2-})\, \langle\bar{q}q\rangle \\
\Pi^{(1)3.1} &= \int d^4x\, e^{ikx} \left[\frac{3\, m_Q^4\, m_q\, N_c}{32\pi^6 x^4}\right] (3K_1^{2-} + 2K_2^{2-})\, \langle\bar{q}q\rangle \\
\Pi^{(2)3.1} &= \int d^4x\, e^{ikx} \left[\frac{3\, m_Q^4\, m_q\, N_c}{64\pi^6 x^4}\right] K_1^{2-}\, \langle\bar{q}q\rangle \\
\Pi^{(0)3.2} &= \int d^4x\, e^{ikx} \left[\frac{m_Q^4\, m_q\, N_c}{64\pi^6 x^4}\right] (99K_1^{2-} + 51K_2^{2-})\, \langle\bar{q}q\rangle \\
\Pi^{(1)3.2} &= \int d^4x\, e^{ikx} \left[\frac{3\, m_Q^4\, m_q\, N_c}{32\pi^6 x^4}\right] (11K_1^{2-} + 5K_2^{2-})\, \langle\bar{q}q\rangle \\
\Pi^{(2)3.2} &= \int d^4x\, e^{ikx} \left[\frac{m_Q^4\, m_q\, N_c}{64\pi^6 x^4}\right] (11K_1^{2-} + 7K_2^{2-})\, \langle\bar{q}q\rangle \\
\Pi^{(0)4} &= \int d^4x\, e^{ikx} \left[\frac{m_Q^4\, N_c^2}{4\pi^8\, x^8}\right] (5K_1^{2-} + 4K_2^{2-}) \\
\Pi^{(1)4} &= \int d^4x\, e^{ikx} \left[\frac{3\, m_Q^4\, N_c^2}{4\pi^8\, x^8}\right] K_1^{2-} \\
\Pi^{(2)4} &= \int d^4x\, e^{ikx} \left[\frac{m_Q^4\, N_c^2}{8\pi^8\, x^8}\right] K_2^{2-}.
\end{aligned}
\tag{2.30}
$$

where m_q^2 terms are eliminated as the expansion at hand is until the order of m_q and $m_q = 0$.

An observation can be made of the pattern the above integrals follow which are all in the form

$$
\Pi^{(s)} = \int d^4x\, e^{ikx} \frac{\alpha_{(\text{ctr})}}{x^{2j}} K_n^2 \tag{2.31}
$$

where $\alpha_{(\text{ctr})}$ is the total coefficient of the term in the correlation function where the quark fields are contracted, (s) the spin, $n = 1, 2$, and $j = 2, 3, 4$.

Using Equation 2.9, the obtained integral is of the form

$$
\begin{aligned}
\Pi_{jn}^{(s)} = \int d^4x\, \frac{\alpha_{(\text{ctr})}}{x^{2j}} \frac{(m_Q)^{2n}}{(-x^2)^n\, 2^{2n+2}} \int_0^\infty dt_1 \int_0^\infty dt_2\, (t_1 t_2)^{(-n-1)} \\
\exp\left[-\frac{m_Q^2}{4t_1} - \frac{m_Q^2}{4t_2} + t_1 x^2 + t_2 x^2 + ikx\right]
\end{aligned}
\tag{2.32}
$$

and changing the configuration space from Minkowskian to Euclidean using Wick rotation, where the transformation is as $x_0 \to ix_0$ and $k_0 \to ik_0$ hence $x^2 \to -x^2$ and $k^2 \to -k^2$ with $kx \to -kx$, the equation becomes

$$\Pi_{jn}^{(s)} = \int d^4x \, \frac{i\alpha_{\text{(ctr)}}}{x^{2j}} \frac{(m_Q)^{2n}}{(x^2)^n \, 2^{2n+2}} \int_0^\infty dt_1 \int_0^\infty dt_2 \, (t_1 t_2)^{(-n-1)} \exp\left[-\frac{m_Q^2}{4t_1} - \frac{m_Q^2}{4t_2} - t_1 x^2 - t_2 x^2 - ikx \right]. \tag{2.33}$$

Using Equation A.2 from the gamma function integral identity, the integral is

$$\Pi_{jn}^{(s)} = \int d^4x \, \frac{i\alpha_{\text{(ctr)}} \, (m_Q)^{2n}}{\Gamma(n+j) 2^{2n+2}} \int_0^\infty dt_1 \int_0^\infty dt_2 \int_0^\infty dt_3 \, (t_1 t_2)^{(-n-1)} t_3^{(n+j-1)} \exp\left[-\frac{m_Q^2}{4t_1} - \frac{m_Q^2}{4t_2} - t_1 x^2 - t_2 x^2 - t_3 x^2 - ikx \right]. \tag{2.34}$$

Gathering the integral into a Gaussian integral over x, d^4x integral can be taken as

$$\begin{aligned} &\int d^4x \, \exp\left[-\frac{m_Q^2}{4} \left(\frac{1}{t_1} + \frac{1}{t_2} \right) - (t_1 + t_2 + t_3) x^2 - ikx \right] = \\ &\int d^4x \, \exp\left[-(t_1 + t_2 + t_3) \left[x + \frac{ik}{2(t_1 + t_2 + t_3)} \right]^2 - \frac{k^2}{4(t_1 + t_2 + t_3)} - \frac{m_Q^2}{4} \left(\frac{1}{t_1} + \frac{1}{t_2} \right) \right] \\ &= \left(\frac{\pi}{t_1 + t_2 + t_3} \right)^2 \exp\left[-\frac{k^2}{4(t_1 + t_2 + t_3)} - \frac{m_Q^2}{4} \left(\frac{1}{t_1} + \frac{1}{t_2} \right) \right] \end{aligned} \tag{2.35}$$

At this point, the integral will be of the form

$$\Pi_{jn}^{(s)} = \frac{i\alpha_{\text{(ctr)}} \pi^2 \, (m_Q)^{2n}}{\Gamma(n+j) 2^{2n+2}} \int_0^\infty dt_1 \int_0^\infty dt_2 \int_0^\infty dt_3 \, \frac{(t_1 t_2)^{(-n-1)} t_3^{(n+j-1)}}{(t_1 + t_2 + t_3)^2} \exp\left[-\frac{k^2}{4(t_1 + t_2 + t_3)} - \frac{m_Q^2}{4} \left(\frac{1}{t_1} + \frac{1}{t_2} \right) \right] \tag{2.36}$$

for which a change of variable is required. Choosing the transformation as $t_1 = tx$,

$t_2 = ty$, and $t_3 = t(1-x-y)$ so that $t_1 + t_2 + t_3 = t$, and the integral is

$$\Pi_{jn}^{(s)} = \frac{i\alpha_{(\text{ctr})}\pi^2 \left(m_Q\right)^{2n}}{\Gamma(n+j)2^{2n+2}} \int_0^\infty \cancel{t^2}\, dt \int_0^1 dx \int_0^{1-x} dy \exp\left[-\frac{k^2}{4t} - \frac{m_Q^2}{4t}\left(\frac{1}{x}+\frac{1}{y}\right)\right] \frac{(xy)^{(-n-1)} t^{(-n+j-3)} (1-x-y)^{n+j-1}}{\cancel{(t)^2}}. \tag{2.37}$$

After the values of n, j, and $\alpha_{(\text{ctr})}$ are placed in, the final integral for the $\Pi^{(s)}$ part of the correlation function is of the form

$$\Pi^{(s)} = c_{(s)} \int_0^\infty \frac{dt}{t^n} \int_0^1 dx \int_0^{1-x} dy \frac{(1-x-y)^a}{(xy)^b} \exp\left[-\frac{k^2}{4t} - \frac{m_Q^2}{4t}\left(\frac{1}{x}+\frac{1}{y}\right)\right] \tag{2.38}$$

where $c_{(s)}$ is the corresponding coefficient for the integral as listed in the Appendix, $n = 0, 1, 2, 3$, $a = 2, 3, 4, 5$, and $b = 2, 3$. Operator product expansion is computed and after the computation of Π^{phen}, Borel transform will be applied on both sides.

2.2.2 Phenomenological Approach

In this approach, the correlation function is examined using the dispersion relation that is constructed from the explicit form of the time-ordered product in Equation 2.2.

$$T\{j_{\alpha\beta}(x) j_{\gamma\delta}^\dagger(0)\} = \theta(x)\, j_{\alpha\beta}(x) j_{\gamma\delta}^\dagger(0) + \theta(-x)\, j_{\gamma\delta}^\dagger(0) j_{\alpha\beta}(x) \tag{2.39}$$

where the Heaviside function is $\theta(x) = 1$ for $x > 0$ and $\theta(x) = 0$ for $x < 0$ and its integral representation is given in the Appendix A Equation A.3. Substituting the complete set of states of the hadron between the currents above, one obtains the expression

$$\langle 0|\, j_{\alpha\beta}(x)\, |h\rangle = \langle 0|\, U^{-1} U j_{\alpha\beta}(x) U^{-1} U\, |h\rangle \tag{2.40}$$

where U is the unitary operator with the properties

$$U(x_0) j_{\alpha\beta}(x) U^{-1}(x_0) = j_{\alpha\beta}(x + x_0) \qquad U(x_0)\, |h\rangle = e^{iq_h x_0}\, |h\rangle \tag{2.41}$$

where q_h is the four momentum of the hadron. Assigning $x_0 = -x$ yields the matrix element

$$\langle 0| j_{\alpha\beta}(x) |h\rangle = e^{-iq_h x} \langle 0| j_{\alpha\beta}(0) |h\rangle . \tag{2.42}$$

All the hadrons in the $|h\rangle$ state are on-shell which means that the state obeys the relativistic equation of motion $E^2 = q_h^2 + m^2$ and the four momentum q_h is constrained to be a timelike vector where one can assign $q_h^2 \equiv t$ with $t \geq 0$. This condition grants the use of the identity

$$\sum_h \int_0^\infty dt \int d^4q\, \theta(p)\delta(q^2 - t)\, \delta^{(4)}(q - q_h) = 1 \tag{2.43}$$

where the sum is over all hadrons. Using the property of Dirac delta to switch the order of sum and integrals, the definition of a scalar function $\Pi(q^2)$ appears as

$$\sum_h \langle 0| j_{\alpha\beta}(0) |h\rangle \langle h| j^\dagger_{\gamma\delta}(0) |0\rangle (2\pi)^4 \delta^{(4)}(q - q_h) \equiv 2\pi\Pi(q^2). \tag{2.44}$$

The spectral function $\Pi(q^2)$ is a function of the four momentum squared q^2 that is Lorenz invariant with mass information of the hadron embedded in $|h\rangle$ only.

Employing all the construction into the correlation function, one gets

$$\begin{aligned}\Pi(k^2) = \int d^4x\, e^{ikx} \int_0^\infty dt\, \Pi(t) \int \frac{d^4q}{(2\pi)^3} \big[& i\theta(x)e^{-iqx}\theta(q)\, \delta(q^2 - t) \\ & + i\theta(-x)e^{iqx}\theta(q)\, \delta(q^2 - t)\big]\end{aligned} \tag{2.45}$$

where the result obtained combined with Equation A.3 can be expressed as the Feynman propagator

$$\begin{aligned}\int \frac{d^4q}{(2\pi)^3} \big[i\theta(x)e^{-iqx}\theta(q)\, \delta(q^2 - t) + i\theta(-x)e^{iqx}\theta(q)\, \delta(q^2 - t)\big] = \\ \int \frac{d^4q}{(2\pi)^4} \frac{e^{-iqx}}{t^2 - q^2} = \Delta_F(x; t).\end{aligned} \tag{2.46}$$

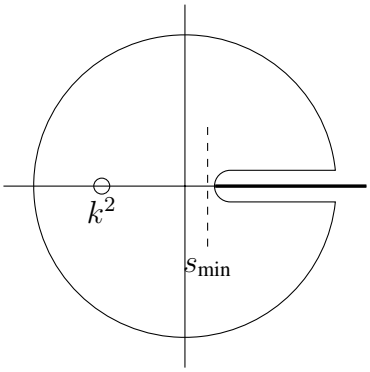

Figure 2.1: Contour over the complex plane t where the branch cut is shown darker.

The correlation function can then be collected as

$$\Pi(k^2) = \int d^4x\, e^{ikx} \int_0^\infty dt\, \Pi(t) \int \frac{d^4q}{(2\pi)^4} \frac{e^{-iqx}}{t^2 - q^2} \tag{2.47}$$

which is the Fourier transformed version of a scalar free field with an arbitrary squared mass t with the weighting function $\Pi(t)$. Taking the integrals over x and q yields

$$\Pi(k^2) = \int_0^\infty dt\, \Pi(t) \frac{1}{t^2 - k^2}. \tag{2.48}$$

As the values of t are constrained by the limits of the integral and as $k^2 > 0$, and $s_{\text{min}} = 0$, mapping the integral into the complex plane of the variable t and integrating over the complex contour shown in Figure 2.1 using Cauchy integral, one can find the above integral as

$$\begin{aligned} \Pi(k^2) &= \frac{1}{2\pi i} \oint dt \frac{\Pi(t)}{t - k^2} \\ &= \frac{1}{2\pi i} \oint_{|t|=R} dt \frac{\Pi(t)}{t - k^2} + \frac{1}{2\pi i} \int_0^R dt \frac{\Pi(t + i\epsilon) - \Pi(t - i\epsilon)}{t - k^2} \end{aligned} \tag{2.49}$$

In the limit $R \to \infty$, the first integral vanishes for when $\lim_{|q^2|\to 0} \sim {}^1\!/_{|q^2|^\epsilon}$ with $\epsilon > 0$, and using the property $\Pi(k^2)$ being real for $k^2 < t_{\text{min}}$ where $t_{\text{min}} = \min\{m_h^2, s_0\}$ and Schwarz reflection principle that is

$$\Pi(k^2 + i\epsilon) - \Pi(k^2 - i\epsilon) = 2i\, \text{Im}\big\{\Pi(k^2)\big\} \quad \text{at } k^2 > t_{\text{min}} \tag{2.50}$$

the dispersion relation is obtained as

$$\Pi(k^2) = \frac{1}{\pi} \int\limits_{t_{\min}}^{\infty} ds \frac{\mathrm{Im}\{\Pi(s)\}}{s - k^2 - i\epsilon}. \tag{2.51}$$

In order to solve the ultraviolet divergence problem of the above expression which results from the unknown subtraction terms and the not well-established spectral functions of the excited and continuum states, an equivalent correlation function is defined as a Taylor expansion as

$$\overline{\Pi}(k^2) = \Pi(k^2) - \Pi(0) \tag{2.52}$$

which makes

$$\overline{\Pi}(k^2) = \frac{k^2}{\pi} \int\limits_{t_{\min}}^{\infty} ds \frac{\mathrm{Im}\{\Pi(s)\}}{s(s - k^2)} \tag{2.53}$$

where

$$\mathrm{Im}\big\{\Pi(k^2)\big\} = \pi\lambda_h^2\, \delta(k^2 - m_h^2) + \pi\rho^h(k^2)\theta(k^2 - s_0) \tag{2.54}$$

with $\lambda_h m_h \epsilon_\mu^{(h)*} = \langle h|\, j_\mu\, |0\rangle$ where λ_h of the partners of $X(3872)$ are defined in the manner below

$$\begin{aligned}
\big\langle 2^{++}\big|\, j^2_{\alpha\beta}\, |0\rangle &= \lambda_2^{2^{++}} \epsilon_{\alpha\beta} \\
\big\langle 1^{++}\big|\, j^2_{\alpha\beta}\, |0\rangle &= \lambda_2^{1^{++}} (\epsilon_\alpha\, k_\beta + \epsilon_\beta\, k_\alpha) \\
\big\langle 0^{++}\big|\, j^2_{\alpha\beta}\, |0\rangle &= \lambda_2^{0^{++}} \left(\frac{k_\alpha k_\beta}{k^2} - \frac{1}{4} g_{\alpha\beta} \right) \\
\big\langle 1^{++}\big|\, j^1_{\alpha\beta}\, |0\rangle &= \lambda_1^{1^{++}} (k_\alpha\, \epsilon_\beta - k_\beta\, \epsilon_\alpha) \\
\big\langle 1^{-+}\big|\, j^1_{\alpha\beta}\, |0\rangle &= \lambda_1^{1^{-+}} \epsilon_{\alpha\beta\delta\gamma}\, k^\delta\, \epsilon'^\gamma \\
\big\langle 0^{++}\big|\, j^0_{\alpha\beta}\, |0\rangle &= \lambda_0^{0^{++}} g_{\alpha\beta}
\end{aligned} \tag{2.55}$$

where the polarization operators ϵ and their identities are defined and explained in

Section A.4 of Appendix A leading the correlation function to become

$$\Pi(k^2) = \frac{k^2\lambda_h^2}{m_h^2(m_h^2-k^2)} + k^2\int_{s_0}^{\infty} ds\frac{\rho^{\text{cont}}(s)}{s(s-k^2)} + \Pi(0) \tag{2.56}$$

and the continuum contribution is eliminated by employing

$$\rho^{\text{cont}}(s) = \rho^{\text{OPE}}(s)\theta(s-s_0) \tag{2.57}$$

and $\Pi(0)$ are the subtraction terms that vanish at the Borel transformation.

To use this representation with the known currents as in Equation 2.29, the projection operators on Equation 2.28 will be used once again and the matrix elements will be defined as in Equation 2.55 that are also given in [72]. The correlation functions with the applied projection operators on Equation 2.2 can then be expressed as

$$\begin{aligned}\Pi^{(2)}_{\alpha\beta;\delta\gamma} = &\frac{\left(\lambda_2^{2^{++}}\right)^2}{k^2-m_{2^{++}}^2}\sum_s \epsilon_{\alpha\beta}\epsilon^*_{\delta\gamma} \\ &+ \frac{\left(\lambda_2^{1^{++}}\right)^2}{k^2-m_{1^{++}}^2}\sum_s (\epsilon_\alpha\, k_\beta + \epsilon_\beta\, k_\alpha)(\epsilon^*_\delta\, k_\gamma + \epsilon^*_\gamma\, k_\delta) \\ &+ \frac{\left(\lambda_2^{0^{++}}\right)^2}{k^2-m_{0^{++}}^2}\sum_s \left(\frac{k_\alpha k_\beta}{k^2} - \frac{1}{4}g_{\alpha\beta}\right)\left(\frac{k_\delta k_\gamma}{k^2} - \frac{1}{4}g_{\delta\gamma}\right)\end{aligned} \tag{2.58}$$

and

$$\begin{aligned}\Pi^{(1)}_{\alpha\beta;\delta\gamma} = &\frac{\left(\lambda_1^{1^{++}}\right)^2}{k^2-m_{1^{++}}^2}\sum_s (k_\alpha\,\epsilon_\beta - k_\beta\,\epsilon_\alpha)(k_\delta\,\epsilon^*_\gamma - k_\gamma\,\epsilon^*_\delta) \\ &+ \frac{\left(\lambda_1^{1^{-+}}\right)^2}{k^2-m_{1^{-+}}^2}\sum_s \epsilon_{\alpha\beta\bar{\alpha}\bar{\beta}}\,k^{\bar{\alpha}}\,\epsilon'^{\bar{\beta}}\epsilon_{\delta\gamma\bar{\delta}\bar{\gamma}}\,k^{\bar{\delta}}\,\epsilon'^{\bar{\gamma}}\end{aligned} \tag{2.59}$$

with

$$\Pi^{(0)}_{\alpha\beta;\delta\gamma} = \frac{\left(\lambda_0^{0^{++}}\right)^2}{k^2-m_{0^{++}}^2} g_{\alpha\beta}g_{\delta\gamma}. \tag{2.60}$$

These representations can be simplified using

$$\begin{aligned}\Pi^{(0)}_{\alpha\beta;\delta\gamma} &= i\int d^4x\, e^{ikx}\,\langle 0|\,T\{j^0_{\alpha\beta}(x)j^{0\dagger}_{\delta\gamma}(0)\}\,|0\rangle \\ &= \frac{(\lambda_0^{0^{++}})^2}{q^2-m^2_{0^{++}}}g_{\alpha\beta}g_{\delta\gamma}\end{aligned} \tag{2.61}$$

$$\begin{aligned}\Pi^{(1)}_{\alpha\beta;\delta\gamma} &= i\int d^4x\, e^{ikx}\,\langle 0|\,T\{j^1_{\alpha\beta}(x)j^{1\dagger}_{\delta\gamma}(0)\}\,|0\rangle \\ &= \frac{(\lambda_1^{1^{++}})^2}{q^2-m^2_{1^{++}}}\kappa^{1^+}_{\alpha\beta\delta\gamma}+\frac{(\lambda_1^{1^{-+}})^2}{q^2-m^2_{1^{-+}}}\kappa^{1^-}_{\alpha\beta\delta\gamma}\end{aligned} \tag{2.62}$$

$$\begin{aligned}\Pi^{(2)}_{\alpha\beta;\delta\gamma} &= i\int d^4x\, e^{ikx}\,\langle 0|\,T\{j^2_{\alpha\beta}(x)j^{2\dagger}_{\delta\gamma}(0)\}\,|0\rangle \\ &= \frac{(\lambda_2^{2^{++}})^2}{q^2-m^2_{2^{++}}}\kappa^{22}_{\alpha\beta\delta\gamma}+\frac{(\lambda_2^{1^{++}})^2}{q^2-m^2_{1^{++}}}\kappa^{21}_{\alpha\beta\delta\gamma}+\frac{(\lambda_2^{0^{++}})^2}{q^2-m^2_{0^{++}}}\kappa^{20}_{\alpha\beta\delta\gamma}.\end{aligned} \tag{2.63}$$

In the equations 2.62 and 2.63, the kappas represent the spin sums as the following

$$\begin{aligned}\kappa^{1^+}_{\alpha\beta\delta\gamma} &= \sum_s (k_\alpha\epsilon_\beta - k_\beta\epsilon_\alpha)(k_\delta\epsilon^*_\gamma - k_\gamma\epsilon^*_\delta) \\ &= -(k_\alpha k_\delta g^\perp_{\beta\gamma} - k_\alpha k_\gamma g^\perp_{\beta\delta} - k_\beta k_\delta g^\perp_{\alpha\gamma} + k_\beta k_\gamma g^\perp_{\alpha\delta})\end{aligned} \tag{2.64}$$

$$\begin{aligned}\kappa^{1^-}_{\alpha\beta\delta\gamma} &= \sum_s \epsilon_{\alpha\beta\bar\alpha\bar\beta}v^{\bar\alpha}\epsilon'^{\bar\beta}\epsilon_{\delta\gamma\bar\delta\bar\gamma}v^{\bar\delta}\epsilon'^{\bar\gamma *} \\ &= -(g^\perp_{\alpha\gamma}g^\perp_{\beta\delta} - g^\perp_{\alpha\delta}g^\perp_{\beta\gamma})\end{aligned} \tag{2.65}$$

$$\begin{aligned}\kappa^{22}_{\alpha\beta\delta\gamma} &= \sum_s \epsilon_{\alpha\beta}\epsilon^*_{\delta\gamma} \\ &= \frac{1}{2}\left(g^\perp_{\alpha\delta}g^\perp_{\beta\gamma} + g^\perp_{\beta\delta}g^\perp_{\alpha\gamma} - \frac{2}{3}g^\perp_{\alpha\beta}g^\perp_{\delta\gamma}\right)\end{aligned} \tag{2.66}$$

$$\begin{aligned}\kappa^{21}_{\alpha\beta\delta\gamma} &= \sum_s (\epsilon_\alpha k_\beta + k_\alpha\epsilon_\beta)(\epsilon^*_\delta k_\gamma + k_\delta\epsilon^*_\gamma) \\ &= -(g^\perp_{\alpha\delta}k_\beta k_\gamma + g^\perp_{\alpha\gamma}k_\beta k_\delta + g^\perp_{\beta\delta}k_\alpha k_\gamma + g^\perp_{\beta\gamma}k_\alpha k_\delta)\end{aligned} \tag{2.67}$$

$$\kappa^{20}_{\alpha\beta\delta\gamma} = \left(\frac{k_\alpha k_\beta}{k^2} - \frac{1}{4}g_{\alpha\beta}\right)\left(\frac{k_\delta k_\gamma}{k^2} - \frac{1}{4}g_{\delta\gamma}\right). \tag{2.68}$$

These structures are orthogonal to each other and $g^\perp_{\mu\nu}$ is the abbreviated form of $\left(g_{\mu\nu} - \frac{k_\mu k_\nu}{k^2}\right)$.

2.2.3 Obtaining Mass

At this point, correlation functions found by the two methods are equated as

$$\Pi^{\text{OPE}}(k^2) = \Pi^{\text{phen}}(k^2) + \text{polynomials in } k^2 \tag{2.69}$$

and both sides will be Borel transformed in order to eliminate the subtraction terms $\Pi(0)$ as in the given form in Section A.3 in Appendix A which brings the resulting correlation functions into the form below.

$$\lambda^2 \, e^{-m_h^2/M^2} = \int_0^{s_0} ds \, \rho^{\text{OPE}}(s) e^{-s/M^2} \tag{2.70}$$

Taking the derivative of both sides with respect to $1/M^2$, one can obtain

$$m_h^2 = \frac{\int_0^{s_0} ds \; s \, \rho^{\text{OPE}}(s) \, e^{-s/M^2}}{\int_0^{s_0} ds \; \rho^{\text{OPE}}(s) \, e^{-s/M^2}}. \tag{2.71}$$

Moving back to the correlation functions at hand, Borel transformation of the OPE side will be carried out to obtain the form below where the $\rho^{\alpha_{\text{int}}}$ represents the spectral density corresponding to the correlation function $\Pi^{(\alpha_{\text{int}})}$ where the form of each $\Pi^{(\alpha_{\text{int}})}$ is given in Appendix B.

$$\hat{B}\left[\Pi^{(\alpha_{\text{int}})}\right] = \int_0^{\infty} ds \; \rho^{(\alpha_{\text{int}})} \, e^{-s/M^2} \tag{2.72}$$

From the OPE side, Equation 2.38 with

$$f(x,y) = \frac{(1-x-y)^a}{x^b y^b} \tag{2.73}$$

will be Borel Transformed as

$$\begin{aligned} \hat{B}\left[\Pi^{(\alpha_{\text{int}})}\right] &= c_{\alpha_{\text{int}}} \int_0^{\infty} \frac{dt}{t^n} \int_0^{1} dx \int_0^{1-x} dy \; f(x,y) \, e^{-s(x,y)/4t} \, \delta\left(\frac{1}{M^2} - \frac{1}{4t}\right) \\ &= c_{\alpha_{\text{int}}} \int_0^{\infty} \frac{dt}{t^n} \int_0^{1} dx \int_0^{1-x} dy \; f(x,y) \, e^{-s(x,y)/4t} \, M^2 \, t \, \delta\left(t - \frac{M^2}{4}\right) \end{aligned} \tag{2.74}$$

where $c_{\alpha_{\text{int}}}$ corresponds to the coefficients listed in the Appendix B and $s(x,y) = \frac{m_Q^2}{4}\left(\frac{1}{x}+\frac{1}{y}\right)$. Taking the integral over t using Delta function will result in

$$\begin{aligned}
\hat{B}\left[\Pi^{(\alpha_{\text{int}})}\right] &= c_{\alpha_{\text{int}}} \int_0^1 dx \int_0^{1-x} dy\; f(x,y)\, e^{-s(x,y)/M^2} \left(\frac{M^2}{4}\right)^{(-n+1)} M^2 \\
&= c_{\alpha_{\text{int}}} \int_0^1 dx \int_0^{1-x} dy\; f(x,y) \left(\frac{2^{-2n+2}}{(M^2)^{n-2}}\right) e^{-s(x,y)/M^2} \\
&= 2^{-2n+2}\, c_{\alpha_{\text{int}}} \int_0^1 dx \int_0^{1-x} dy\; f(x,y) \left(\frac{1}{(M^2)^{n-2}}\right) e^{-s(x,y)/M^2} \\
&= 2^{-2n+2}\, c_{\alpha_{\text{int}}} \int_0^\infty ds \int_0^1 dx \int_0^{1-x} dy\; f(x,y) \left(\frac{e^{-s/M^2}}{(M^2)^{n-2}}\right) \delta(s - s(x,y)) \\
&= 2^{-2n+2}\, c_{\alpha_{\text{int}}} \int_0^\infty ds\; e^{-s/M^2} \frac{1}{(M^2)^{n-2}} \int_0^1 dx \int_0^{1-x} dy\; f(x,y)\, \delta(s - s(x,y)).
\end{aligned} \tag{2.75}$$

To determine the spectral function, the factor multiplying the exponential in the integrand of the s integral should be independent of M^2. Hence OPE side will be examined in three branches from this point on depending on the form of M^2. The differentiation will be over the variable n, the power of t in the Equation 2.38. The first type is the group where $n < 2$.

For $n < 2$, the equation at hand is in the form

$$\int_0^\infty ds\; e^{-s/M^2} \left(M^2\right)^k \tilde{\rho}(s) \tag{2.76}$$

with $k > 0$ for $n < 2$.

The substitute spectral density $\tilde{\rho}(s)$ corresponds to the k^{th} derivative of the actual spectral density as

$$\tilde{\rho}(s) = \left(\frac{d}{ds}\right)^k \rho(s). \tag{2.77}$$

Then, Equation 2.75 can be represented as

$$\hat{B}\left[\Pi^{(\alpha_{\text{int}})}\right] = \int_0^\infty ds\; e^{-s/M^2}\left(M^2\right)^k \left(\frac{d}{ds}\right)^k \rho(s). \tag{2.78}$$

Applying integration by parts, the integral transforms into

$$\begin{aligned}\hat{B}\left[\Pi^{(\alpha_{\text{int}})}\right] = e^{-s/M^2}\left(M^2\right)^k \left(\frac{d}{ds}\right)^{k-1} \rho(s)\Big|_{s=0}^{\infty} \\ + \int_0^\infty ds\; e^{-s/M^2}\left(M^2\right)^{k-1} \left(\frac{d}{ds}\right)^{k-1} \rho(s)\end{aligned} \tag{2.79}$$

At the boundary $s \to \infty$, exponential brings the term into zero and at $s = 0$, the boundary condition will be assumed as

$$\left(\frac{d}{ds}\right)^n\Big|_{s=0} \rho(s) = 0 \qquad 0 \le n \le k-1. \tag{2.80}$$

In the case $n = 0$, $k = 1$, Equation 2.79 becomes

$$\hat{B}\left[\Pi^{(\alpha_{\text{int}})}\right] = 0 + \int_0^\infty ds\; e^{-s/M^2}\rho(s) \tag{2.81}$$

which is the desired form. This makes

$$\begin{aligned}\tilde{\rho}(s) &= \int_0^1 dx \int_0^{1-x} dy\; f(x,y)\,\delta(s - s(x,y)) = \frac{d}{ds}\rho(s) \\ \rho(s) &= \int_0^1 dx \int_0^{1-x} dy\; f(x,y)\,\Theta(s - s(x,y)).\end{aligned} \tag{2.82}$$

In the case $n = 1$, $k = 2$, Equation 2.79 becomes

$$\begin{aligned}\hat{B}\left[\Pi^{(\alpha_{\text{int}})}\right] = e^{-s/M^2}\left(M^2\right)^2 \left(\frac{d}{ds}\rho(s)\right)\Big|_{s=0}^{\infty} \\ + \int_0^\infty ds\; e^{-s/M^2} M^2 \left(\frac{d}{ds}\rho(s)\right).\end{aligned} \tag{2.83}$$

Using the same boundary conditions as in $n = 0$ case as

$$e^{-s/M^2}\Big|_{s\to\infty} = 0 \qquad \frac{d}{ds}\rho(s)\Big|_{s=0} = 0 \tag{2.84}$$

Borel transform of the correlation function becomes

$$\hat{B}\left[\Pi^{(\alpha_{\text{int}})}\right] = e^{-s/M^2}\,\rho(s)\Big|_{s=0}^{\infty} + \int_0^{\infty} ds\; e^{-s/M^2}\,\rho(s). \tag{2.85}$$

Since

$$\begin{aligned}\rho(s) &= \frac{1}{\Gamma(n-1)}\int_0^s d\alpha\;\,(s-\alpha)^{n-1}\,\tilde{\rho}(s) \\ &= \frac{1}{\Gamma(n-1)}\int dx\int dy\; f(x,y)\;(s-s(x,y))^{n-1}\;\theta(s-s(x,y))\end{aligned} \tag{2.86}$$

is the solution for the differential equation below with the boundary conditions in Equation 2.80

$$\tilde{\rho}(s) = \left(\frac{d}{ds}\right)^n \rho(s). \tag{2.87}$$

Meaning that

$$\begin{aligned} n=0;\quad \rho(s) &= \int_0^s d\alpha\;(s-\alpha)\int_0^1 dx\int_0^{1-x} dy\; f(x,y)\,\delta(\alpha - s(x,y)) \\ n=1;\quad \rho(s) &= \int_0^s d\alpha\int_0^1 dx\int_0^{1-x} dy\; f(x,y)\,\delta(\alpha - s(x,y)). \end{aligned} \tag{2.88}$$

For the second group of n, the value 2 is taken. The form of the Borel transformed integral is in the desired form as below.

$$\hat{B}\left[\Pi^{(\alpha_{\text{int}})}\right] = 2^{-2} c_{\alpha_{\text{int}}} \int_0^{\infty} ds\; e^{-s/M^2}\,\rho(s) \tag{2.89}$$

with

$$n = 2; \quad \rho(s) = \int_0^1 dx \int_0^{1-x} dy \; f(x,y)\, \delta(s - s(x,y)). \tag{2.90}$$

For the last group, the values remaining are $n > 2$ of which $n = 3$ is the last. For which Equation 2.75 is

$$\hat{B}\left[\Pi^{(\alpha_{\text{int}})}\right] = 2^{-4} c_{\alpha_{\text{int}}} \int_0^\infty ds \; \frac{1}{M^2}\, e^{-s/M^2} \int_0^1 dx \int_0^{1-x} dy \; f(x,y)\, \delta(s - s(x,y)) \tag{2.91}$$

using the exponential, $1/M^2$ term can be written as the derivative of the exponential

$$\hat{B}\left[\Pi^{(\alpha_{\text{int}})}\right] = 2^{-4} c_{\alpha_{\text{int}}} \int_0^\infty ds \left(-\frac{d}{ds}\, e^{-s/M^2}\right) \int_0^1 dx \int_0^{1-x} dy \; f(x,y)\, \delta(s - s(x,y)). \tag{2.92}$$

Once again, applying integration by parts on the integral leads to

$$-e^{-s/M^2}\, \rho(s)\Big|_{s=0}^{\infty} + \int_0^\infty ds \; e^{-s/M^2} \frac{d}{ds} \left[\int_0^1 dx \int_0^{1-x} dy \; f(x,y)\, \delta(s - s(x,y))\right] \tag{2.93}$$

where the first term vanishes when the previously introduced boundary conditions on the spectral density are employed here as well. Then,

$$\hat{B}\left[\Pi^{(\alpha_{\text{int}})}\right] = 2^{-4} c_{\alpha_{\text{int}}} \int_0^\infty ds \; e^{-s/M^2} \frac{d}{ds} \left[\int_0^1 dx \int_0^{1-x} dy \; f(x,y)\, \delta(s - s(x,y))\right] \tag{2.94}$$

which means

$$n = 3; \quad \rho(s) = \frac{d}{ds} \left[\int_0^1 dx \int_0^{1-x} dy \; f(x,y)\, \delta(s - s(x,y))\right]. \tag{2.95}$$

As the Borel transformed integrals are in the desired form, one can proceed into the continuum subtraction. For the correlation functions with $n = 0, 1, 2$, only the upper

boundaries, infinity, will be transformed into s_0, but for $n = 3$, one has the Equation 2.94 upon which an integration by parts yields

$$\begin{aligned}\hat{B}\left[\Pi^{(\alpha_{\text{int}})}\right] = 2^{-4} c_{\alpha_{\text{int}}} &\left[e^{-s/M^2} \int_0^1 dx \int_0^{1-x} dy\ f(x,y)\,\delta(s - s(x,y)) \right]_{s=0}^{s=s_0} \\ &+ 2^{-4} c_{\alpha_{\text{int}}} \int_0^{s_0} ds\ \frac{1}{M^2}\, e^{-s/M^2} \int_0^1 dx \int_0^{1-x} dy\ f(x,y)\,\delta(s - s(x,y)).\end{aligned} \tag{2.96}$$

Explicit forms and results of these integrals and their corresponding derivatives which are with respect to $1/M^2$ are given in the Appendix C with the corresponding coefficients in Appendix B. Mass values are to be found by dividing the derivatives into the original equation as in Equation 2.71.

CHAPTER 3

COMPUTATIONAL ANALYSIS

The analysis starts with the construction at the last step of the previous chapter in Equation 2.71 as repeated below where the numerical analysis includes a random data set for the variables.

$$m_h^2 = \frac{\int_0^{s_0} ds\ s\,\rho^{\text{OPE}}(s)\,e^{-s/M^2}}{\int_0^{s_0} ds\ \rho^{\text{OPE}}(s)\,e^{-s/M^2}} \tag{3.1}$$

The computational analysis of squared mass values is carried out on Wolfram Mathematica 12.0.0. In the program, the operator product expansion includes higher dimension terms such as gluon condensate and mixed quark-gluon condensate. The values of examined variables are randomly chosen between the ranges given in [40] with additional restrictions in order to eliminate unphysical values of the resulting squared mass in the Table 3.1. The first of the additional restrictions are on M^2 on the lower bound which is increased from $0\ GeV^2$ to $3\ GeV^2$. Second restriction is on the lower bound of s_0 which is increased from $14\ GeV^2$ to $16\ GeV^2$. The data is generated for 1401 sets, one being the control with the previous study at [72]. One of the sets resulted in an indeterminate value for the mass and hence discarded leaving a total of 1400 sets. Histograms in Figures 3.1-3.18 are generated using Python 3.7.3. Each histogram contains a legend consisting of mean (μ), standard deviation (σ), bin size and the number of data around the ranges of the plot which are $[0, 30]\ GeV^2$ for Figures 3.1, 3.3, 3.5, 3.7, 3.9, and 3.11 and $[-5, 5]\ GeV^2$ for Figures 3.13, 3.15, and 3.17. Over each squared mass histogram, the Gaussian distribution with the same mean and standard deviation values are plotted in red. Squared mass values below $2\ GeV^2$ are discarded from the data sets in order to examine physical results.

Variable	Ranges	Control
s_0	$16 - 22\ GeV^2$	$18\ GeV^2$
M^2	$3 - 25\ GeV^2$	$8\ GeV^2$
$\langle qq \rangle$	$0.0143 \pm 0.0012\ GeV^3$	$0.0143\ GeV^3$
m_0^2	$0.80 \pm 0.08\ GeV^2$	$0.80\ GeV^2$
$\langle G_{\mu\nu} G^{\mu\nu} \rangle$	$0.474 \pm 0.015\ GeV^4$	$0.474\ GeV^4$

Table 3.1: Randomisation ranges for the corresponding variables with the control values

Highest peaks of each plot are separately studied in Figures 3.2, 3.4, 3.6, 3.8, 3.10, 3.12, 3.14, 3.16, and 3.18. Each histogram has vertical axes as the density of collected data corresponding to the squared mass values at the horizontal axes in GeV^2. All plots are fitted and the density of each histogram is scaled to 1. On each histogram, ranges of high peaks are drawn dashed. Over each comparison histogram, the Gaussian distribution with the same mean and standard deviation values are plotted in red. For each histogram, details of the distributions and possible reasons for the unexplained peaks and heavy tails are explained. A common observation from the full range histograms is the value of the highest possible J from each correlation function resulted in two peaks with a heavy tail towards the lower values whose heavy tails are reduced by introducing aforementioned range restrictions as in Figures 3.1, 3.7, and 3.11.

When the histogram in Figure 3.1 is inspected, the distribution can be seen to form two peaks with the mean value $15.6\ GeV^2$ with the standard deviation of $1.71\ GeV^2$ which one might consider high concerning the mean value. However, the reason behind the standard deviation being higher than expected is mainly due to the few number of data obtained. Collection of additional data may merge both peaks into a single one and form a less deviated Gaussian.

For the histogram in the Figure 3.2, the mean value is $14.3\ GeV^2$ with the standard deviation of $0.739\ GeV^2$ which is considerably small due to the exclusion of multiple peaks while the mean value is close to the one from the full range distribution in Figure 3.1. The distribution is close to a beta distribution and to obtain a smoother function for this distribution, one might have to inspect the behaviour of the sets

resulting in this distribution and include more data.

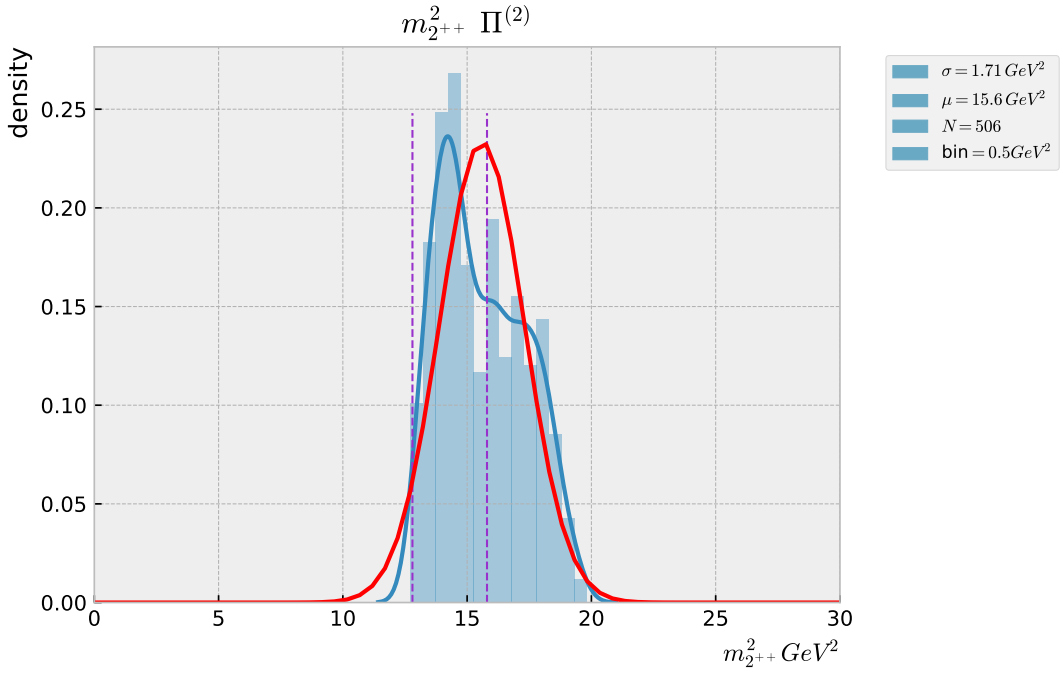

Figure 3.1: Distribution of $m^2_{2^{++}}$ values from $\Pi^{(2)}$

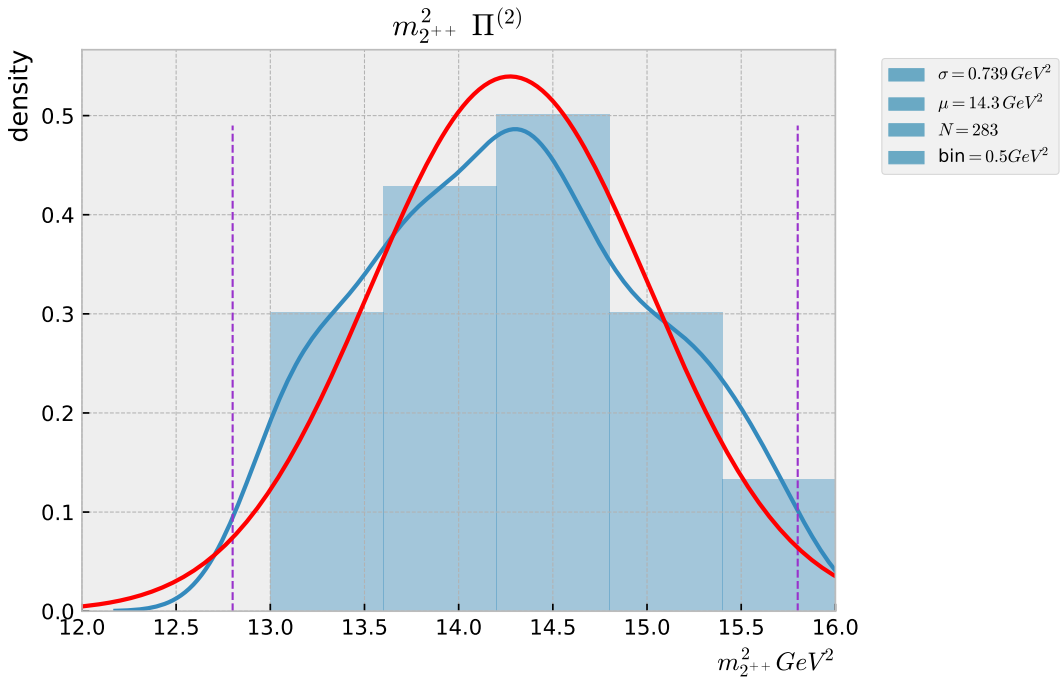

Figure 3.2: Highest peak distribution of $m^2_{2^{++}}$ values from $\Pi^{(2)}$

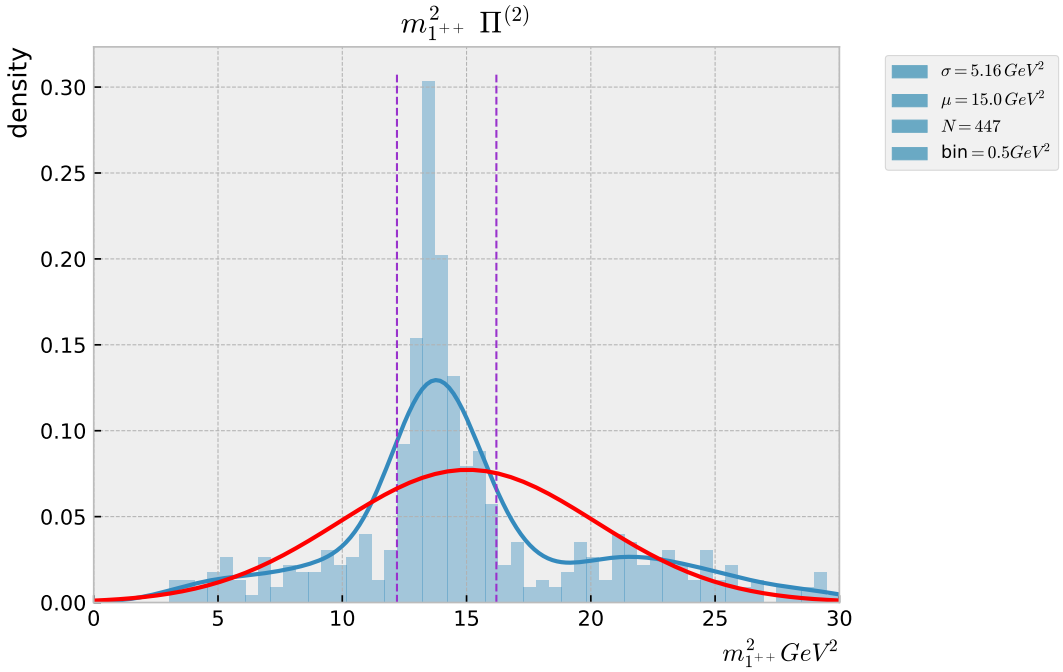

Figure 3.3: Distribution of $m^2_{1^{++}}$ values from $\Pi^{(2)}$

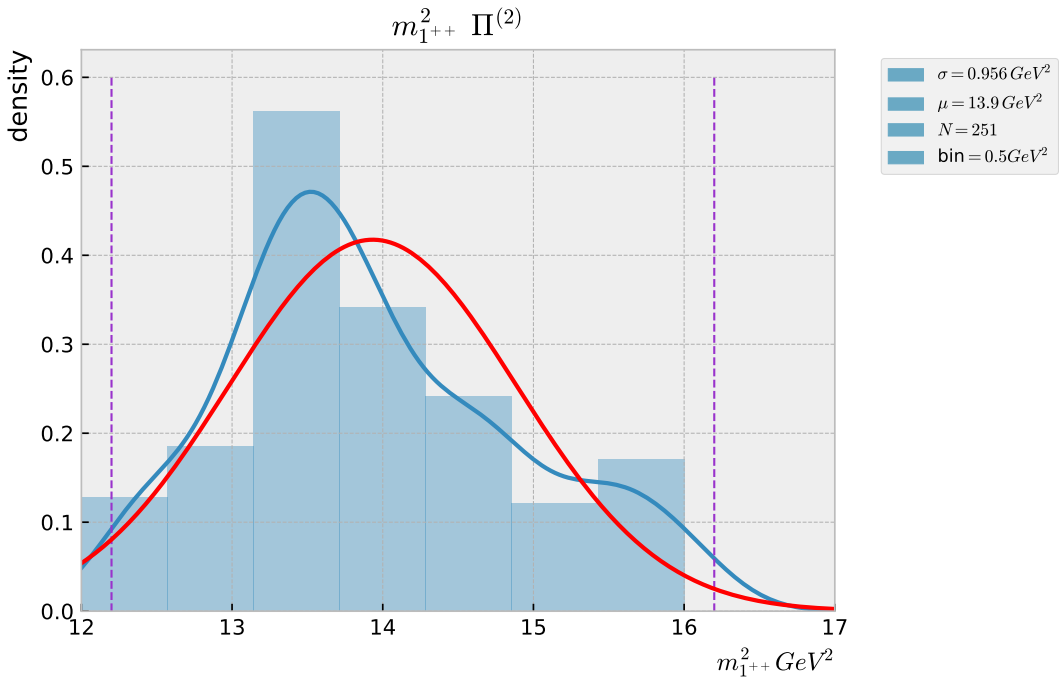

Figure 3.4: Highest peak distribution of $m^2_{1^{++}}$ values from $\Pi^{(2)}$

Examining Figure 3.3, one can observe the mean value as $15.0\ GeV^2$ and standard deviation as $5.16\ GeV^2$ with the highest peak range including the experimentally observed value of $14.99\ GeV^2$. Similar to the previous graph, the high value of standard deviation might have the same underlying reasons as before with the choices of arguable randomness of the software used. While the distribution is considerably more flat compared to other squared mass values obtained from the same correlation function and from $\Pi^{(1)}$, it should be acknowledged that $m^2_{1^{++}}$ values obtained from $\Pi^{(1)}$ have less kurtosis and the distribution here resembles a collection of uniform distribution, which seems to be resulting in the increase of standard deviation value as well hence widening the Gaussian distribution, along with a Gaussian one.

In the Figure 3.4, one can observe the mean value as $13.9\ GeV^2$ and standard deviation as $0.956\ GeV^2$ while the peak range includes the experimental value of $14.99\ GeV^2$. The distribution again has heavy tails and the behaviour of these tails might require additional data sets, as well as a further study on the obtained sets and their corresponding integrals of Borel transformed correlation functions and their relation with corresponding derivatives in order to reach a more conclusive distribution.

In Figure 3.5, one can observe the mean and standard deviation values as $16.9\ GeV^2$ and $3.71\ GeV^2$, respectively. Again, the standard deviation value is similarly large to which similar underlying factors might be contributing. Nevertheless, the fact that $\Pi^{(0)}$ results showing a higher peak and a lower standard deviation with a similar skewness towards the higher end might show a relation between the degeneracy of spin and distribution of squared mass values.

For the highest peak of $m^2_{0^{++}}$ in the Figure 3.6, first observation is the mean and standard deviation values as $15.9\ GeV^2$ and $1.55\ GeV^2$, respectively. The theoretical value can be seen in the highest peak and therefore included in the peak ranges. However, the inclusion of ranges $16.5 - 18.5$ can be seen to increase the value of standard deviation and the mean value. However, additional data may help to merge the two peaks into one and create a true Gaussian distribution.

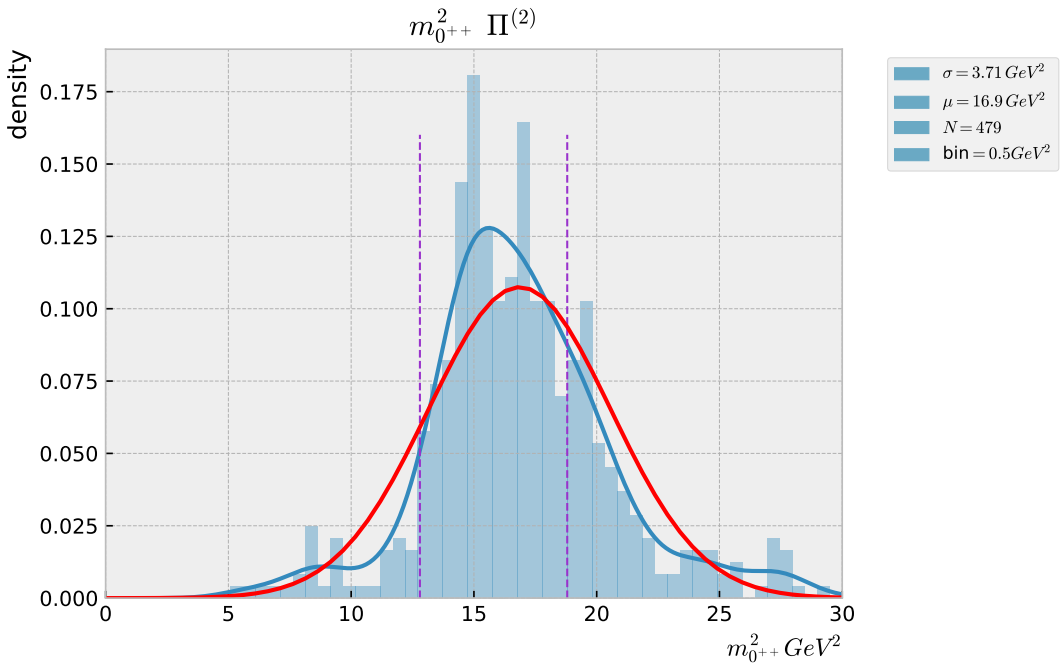

Figure 3.5: Distribution of $m^2_{0^{++}}$ values from $\Pi^{(2)}$

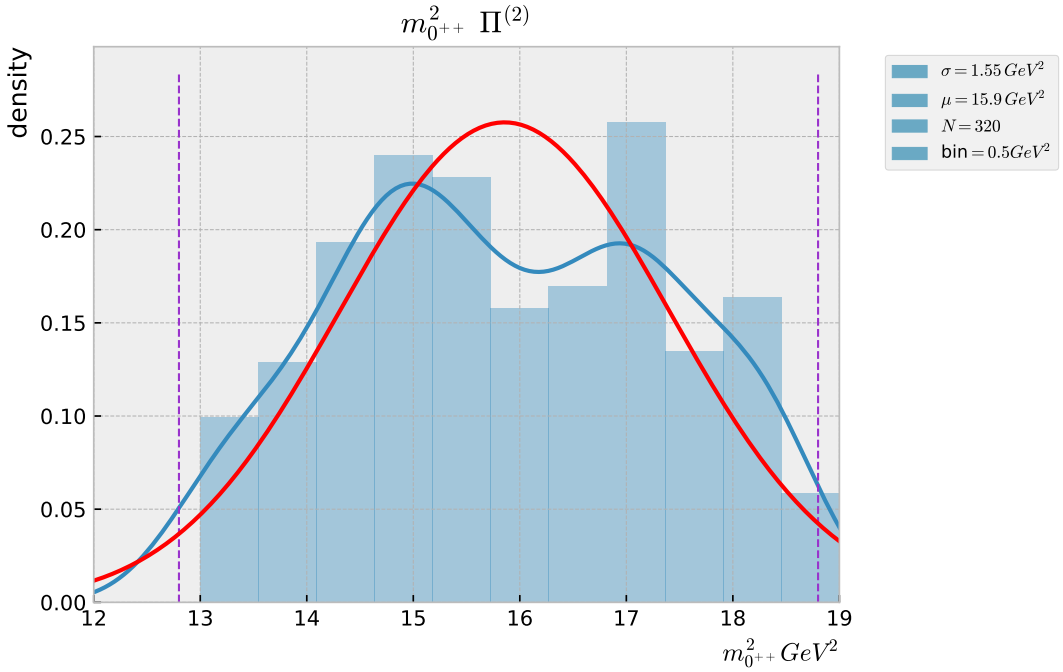

Figure 3.6: Highest peak distribution of $m^2_{0^{++}}$ values from $\Pi^{(2)}$

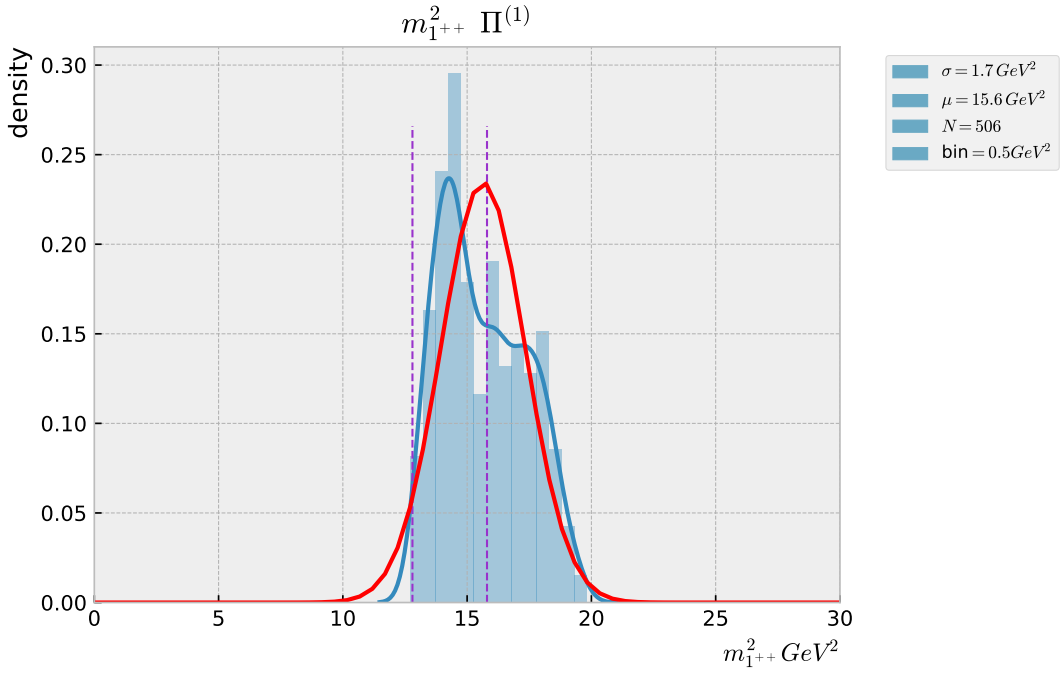

Figure 3.7: Distribution of $m^2_{1^{++}}$ values from $\Pi^{(1)}$

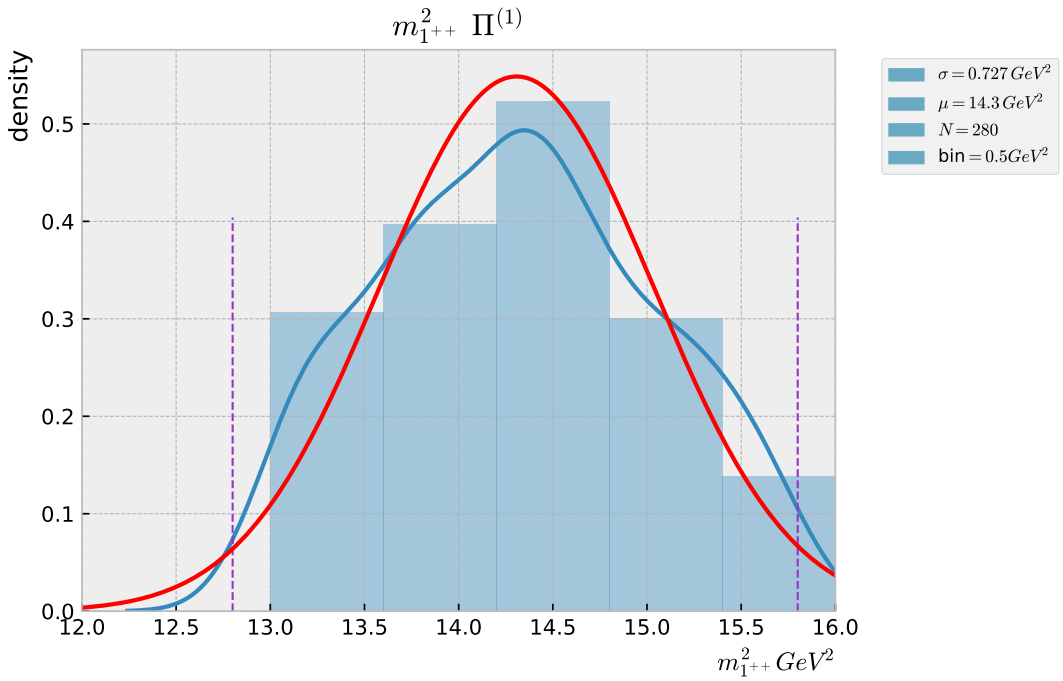

Figure 3.8: Highest peak distribution of $m^2_{1^{++}}$ values from $\Pi^{(1)}$

Figure 3.7 represents the $m^2_{1^{++}}$ values with mean value $15.6\ GeV^2$ and standard deviation of $1.7\ GeV^2$. This is a more peaked Gaussian curve where the highest peak range includes the experimental value of $14.99\ GeV^2$ with no dense tails and as mentioned before, shows a skewing towards higher values. The skewing might be due to the distribution of sets favouring a higher result for the Borel transformed correlation function and lower result for its derivative.

Next, Figure 3.8 shows the $m^2_{1^{++}}$ values from $\Pi^{(1)}$ with mean value $14.3\ GeV^2$ and standard deviation of $0.727\ GeV^2$ with more than half of the data sets from the full range and including the experimental value of $14.99\ GeV^2$ which is closer than half σ to the mean value. The distribution shows a similarity to a Gaussian distribution with some noise which may reduce after a study of additional data. Again, the behaviour of these formations indicates the need for extra data collection and further study of the random variable sets.

Distribution of $m^2_{1^{-+}}$ values from $\Pi^{(1)}$ in Figure 3.9 shows a distinct Gaussian curve with the mean value of $15.6\ GeV^2$ and standard deviation of $5.35\ GeV^2$ and again a second peak towards the higher end of the graph. As there is no other current resulting in this degeneracy to find another $m^2_{1^{-+}}$ from the correlation function, comparison to other $m^2_{1^{-+}}$ results from the same set of values for the variables is not possible at the moment.

Inspecting Figure 3.10 along with the full range Figure 3.9, one can observe the discrete separation of each peak where the highest one shows a kurtosis behaviour. The standard deviation of the highest peak being higher than most of the highest peak distributions here might indicate the sets resulting in the high end and low-end tails of the full range distribution might be disrupting the result. The issue can be solved by examining the Borel transformed correlation function and its derivative along with the sets resulting in the tail peaks.

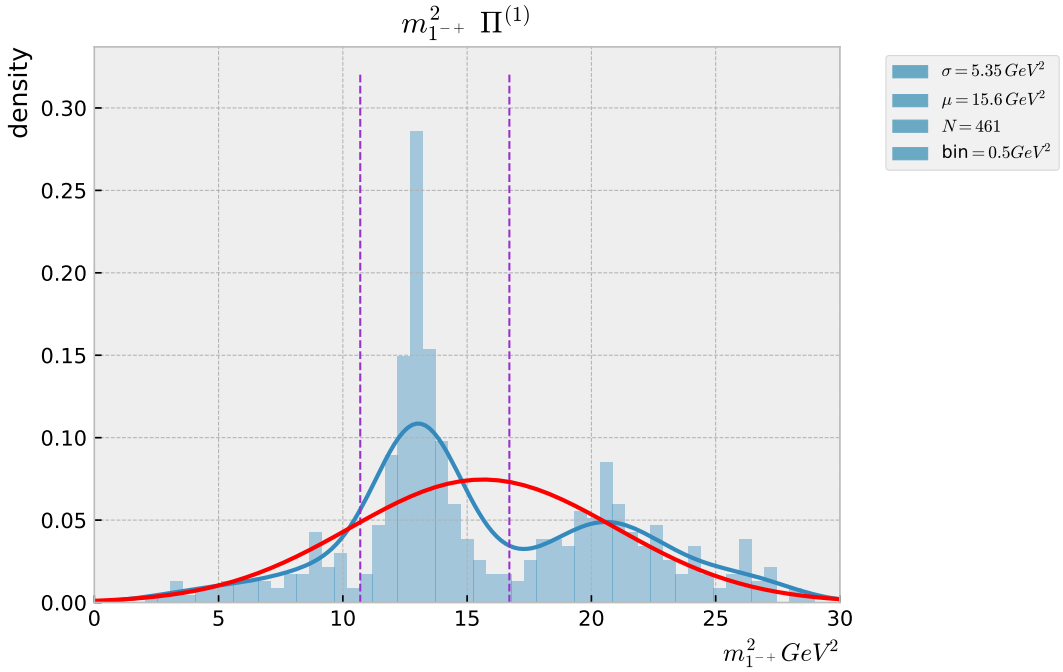

Figure 3.9: Distribution of $m^2_{1^{-+}}$ values from $\Pi^{(1)}$

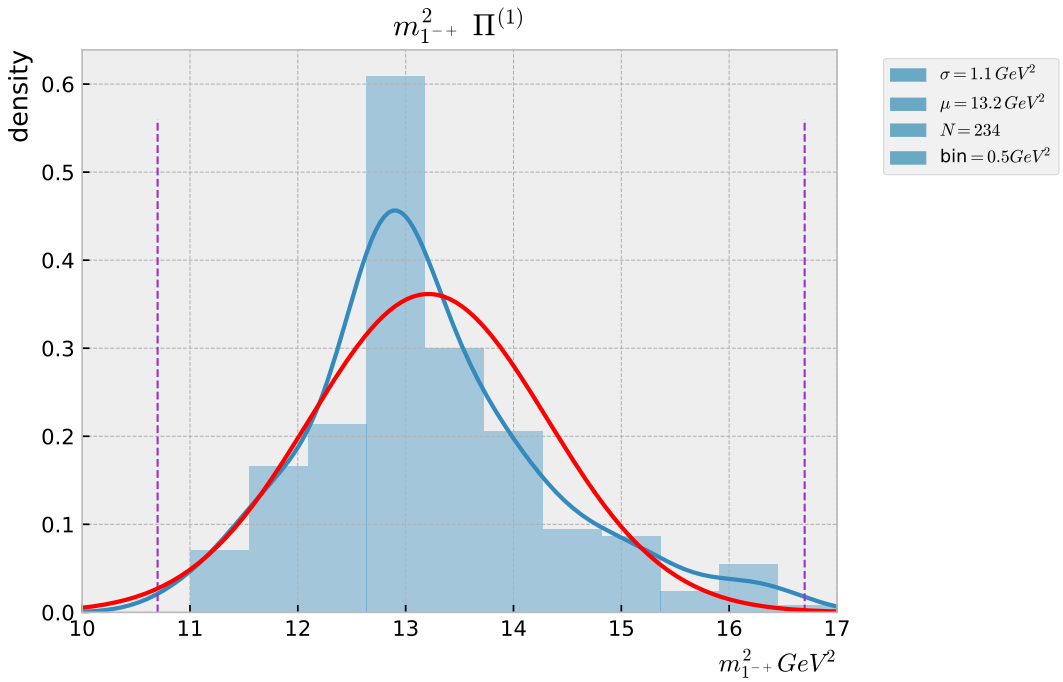

Figure 3.10: Highest peak distribution of $m^2_{1^{-+}}$ values from $\Pi^{(1)}$

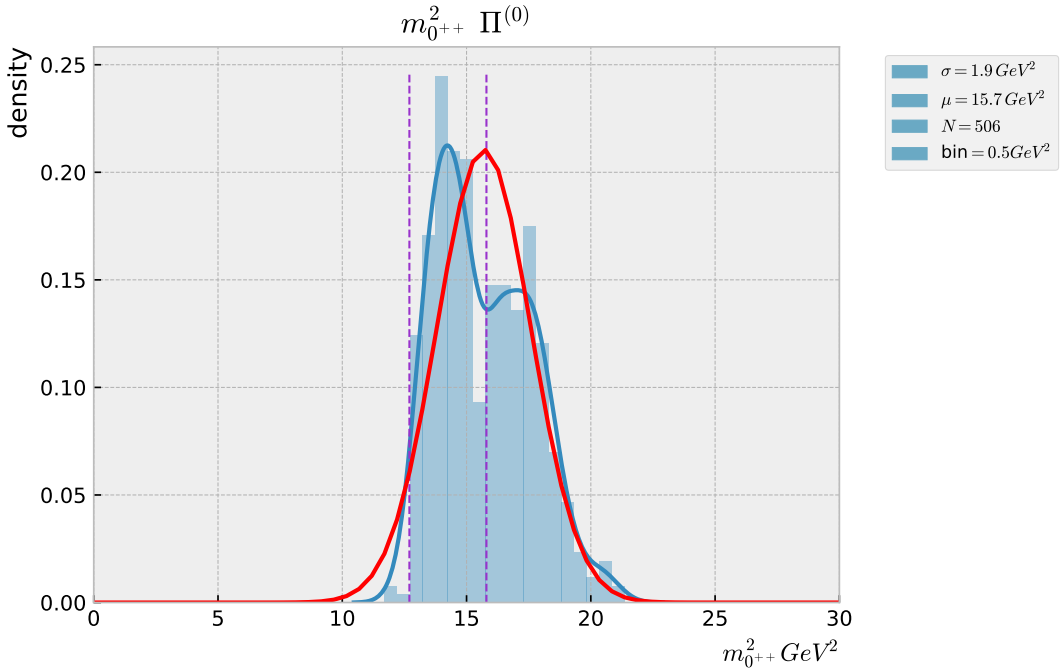

Figure 3.11: Distribution of $m^2_{0^{++}}$ values from $\Pi^{(0)}$

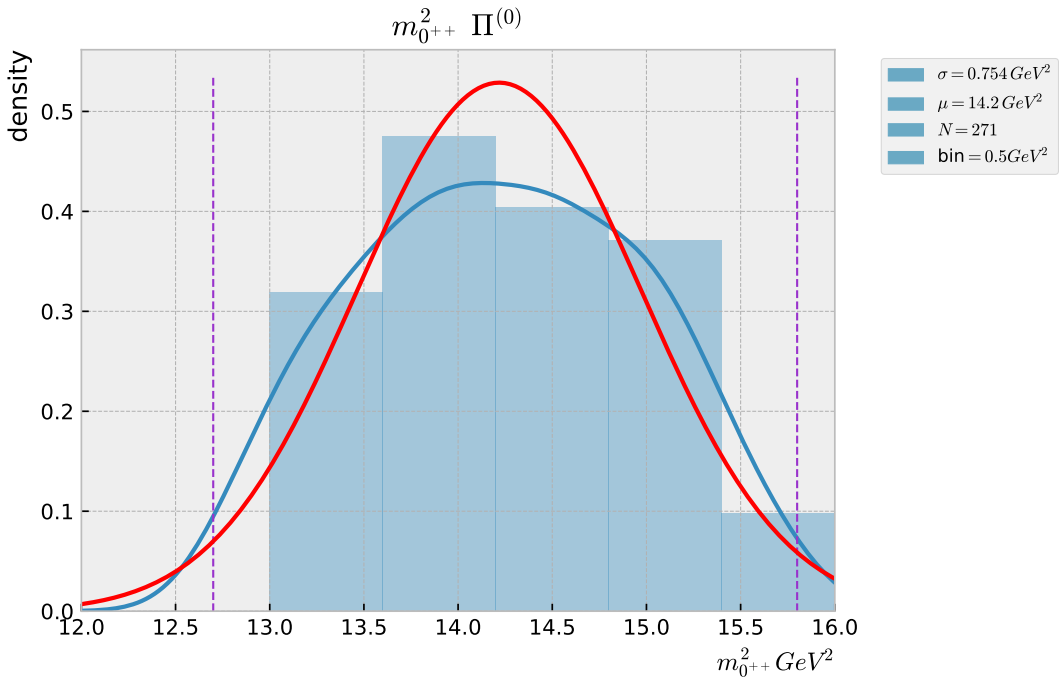

Figure 3.12: Highest peak distribution of $m^2_{0^{++}}$ values from $\Pi^{(0)}$

In the distribution of $m^2_{0^{++}}$ from $\Pi^{(0)}$, one can notice the mean value as $15.7\ GeV^2$ and the standard deviation value as $1.9\ GeV^2$. The aforementioned skew towards the higher end with a considerably higher peak compared to the results obtained from $\Pi^{(2)}$ can be observed as well as a similar pattern with the Figures 3.7 and 3.1. This might indicate that the degeneracy might be effective in the properties of the distribution of squared mass values or that the maximum value the spin can take from the current determines the distribution of the squared mass values.

For the Figure 3.12, one can see the standard deviation value as $0.754\ GeV^2$ and the mean value as $14.2\ GeV^2$. Including more than half of the sets constructed for the full range, the distribution shows a bell-shaped curve with deviations which might be smoothed by generating more sets to study the squared mass further. The fact that the highest peak and the values expected in the literature [73, 74] are in the same range shows the effect of the error margins on the randomised variables are in decrease.

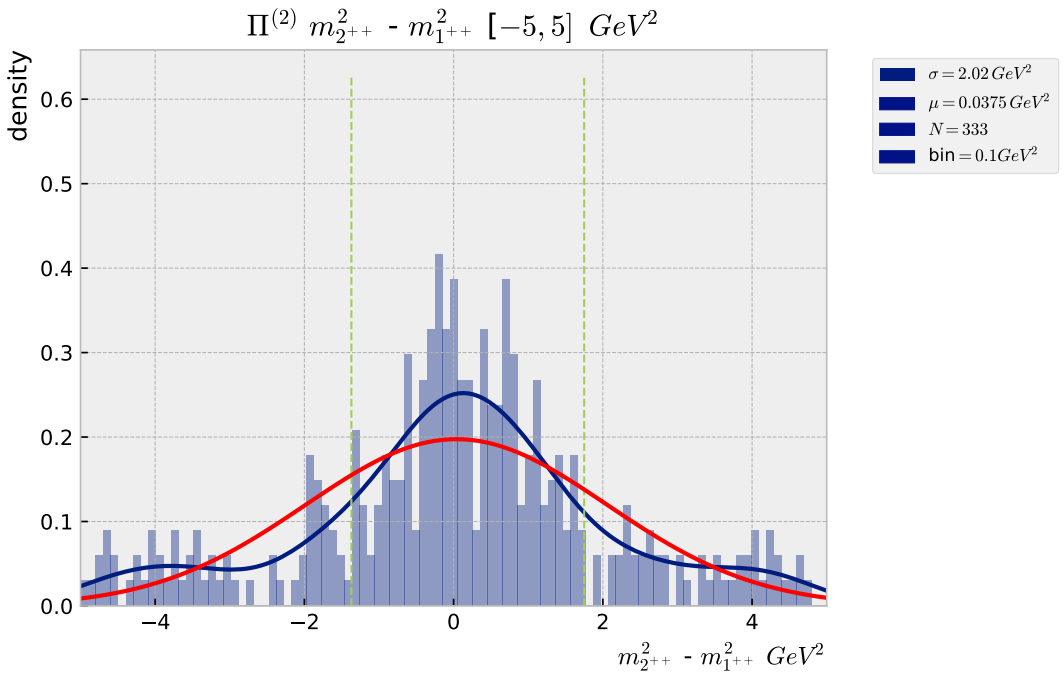

Figure 3.13: Distribution of $m^2_{2^{++}} - m^2_{1^{++}}$ values from $\Pi^{(2)}$

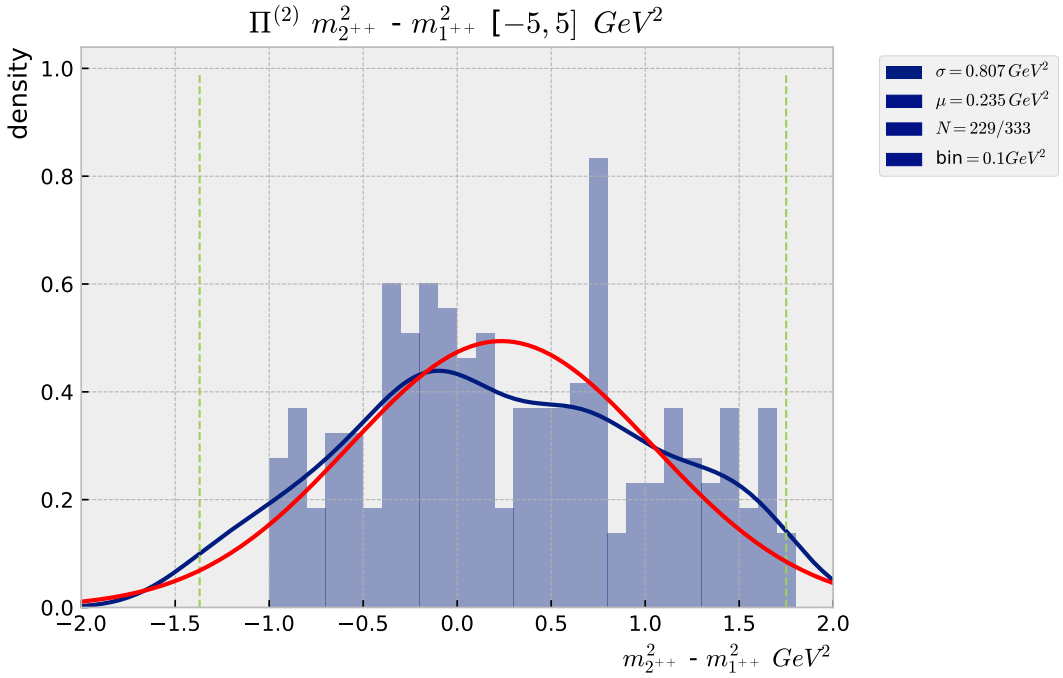

Figure 3.14: Highest peak distribution of $m^2_{2^{++}} - m^2_{1^{++}}$ values from $\Pi^{(2)}$

First of the comparison histograms in Figure 3.13 shows a small mean value as 0.0375 GeV^2 and considerably small standard deviation with value 2.02 GeV^2 compared to the individual squared mass distributions of each constituent. The distribution shows uniform like tails towards each end which may be due to the incompatible derivative of the Borel transformed correlation functions with themselves in the same sets. For this reason, a further study of these sets and correlation functions may be due. Nonetheless, the distribution is almost symmetrical which might indicate that the masses of these partners of $X(3872)$ can be found in the same range hence dynamics of the $X(3872)$ particles obtained in the same interaction with the same mass may follow two different pathways afterwards.

In Figure 3.14, the mean value 0.235 GeV^2 being larger than the full ranged comparison distribution is due to the fact that the highest peak spans more of the positive values than the negative ones. The reason for that is seemingly due to the data obtained for the $m^2_{2^{++}}$ shows more peaking trend while $m^2_{1^{++}}$ tends to span more uniform distribution towards the higher end of the curve. In the legend, it can be seen that most of the data of the full range distribution are present while the standard deviation is considerably smaller although the distribution shows a smaller peak and heavy tails.

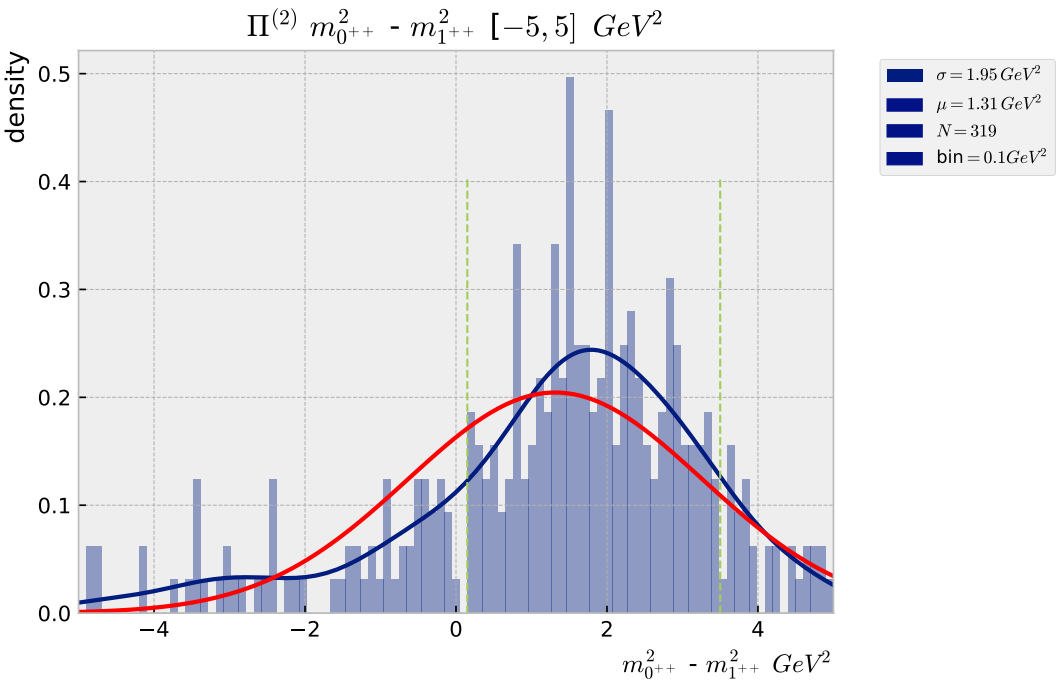

Figure 3.15: Distribution of $m^2_{0^{++}} - m^2_{1^{++}}$ values from $\Pi^{(2)}$

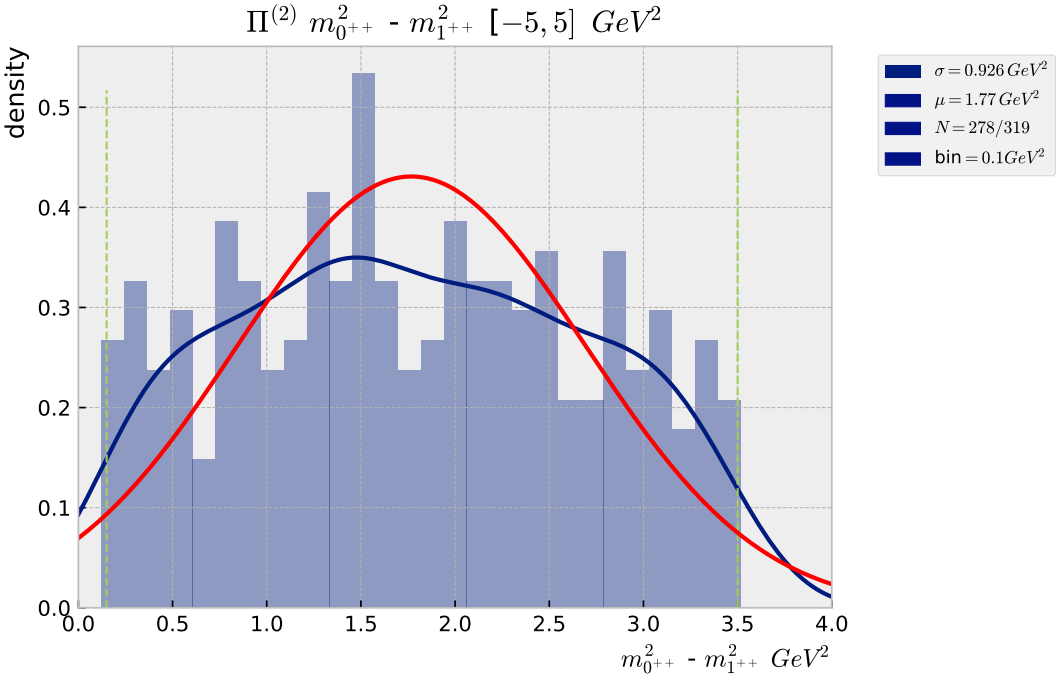

Figure 3.16: Highest peak distribution of $m^2_{0^{++}} - m^2_{1^{++}}$ values from $\Pi^{(2)}$

In the second comparison graph in Figure 3.15, one can observe a skewed distribution with mean value of $1.31\ GeV^2$ and standard deviation of $1.95\ GeV^2$. The reason why the standard deviation value is higher than the mean may be due to the skewed nature of the distribution and might be due to $m^2_{0^{++}}$ being around $1\ GeV$ larger than $m^2_{1^{++}}$. Nevertheless, the distribution skewing towards the higher end may simply be due to the distribution of $m^2_{0^{++}}$ skewing towards the higher end and $m^2_{1^{++}}$ towards the lower end from $\Pi^{(2)}$. As the smallest number of data sets are obtained here, again a further inspection of the sets and correlation functions might be fruitful.

Figure 3.16 shows the mean value of $1.77\ GeV^2$ which is higher than the mean value of the full distribution because the highest peak shows $m^2_{0^{++}}$ values obtained are higher compared to $m^2_{1^{++}}$ values as can be seen in the Figures 3.5 and 3.3. While including most of the data from the full range, the standard deviation obtained is noticeably smaller than the full range of the differences albeit the distribution showing more of a uniform configuration.

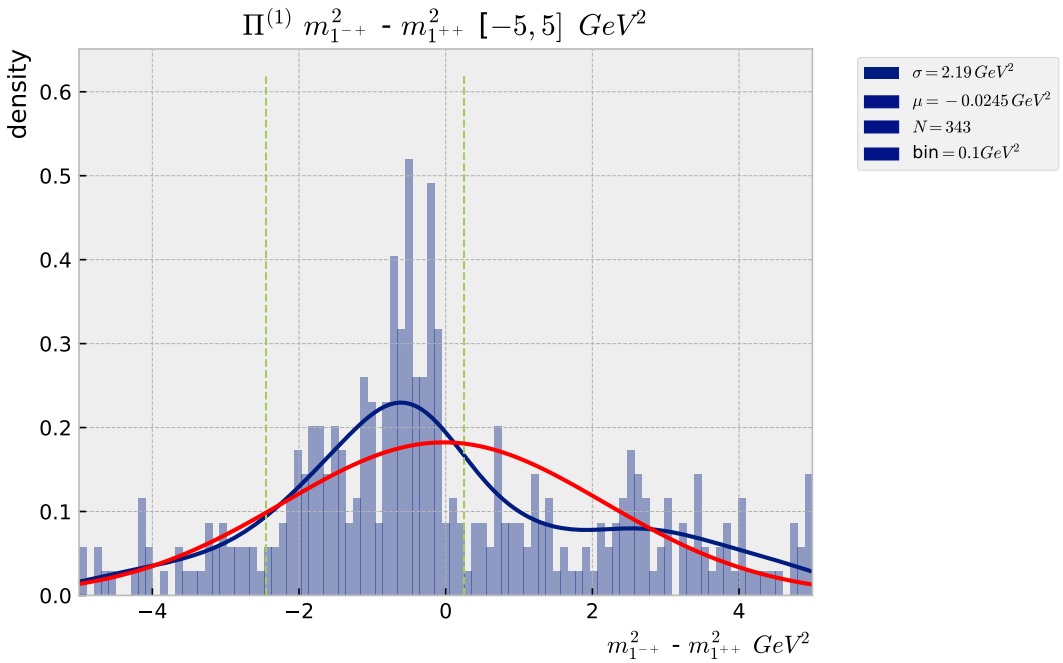

Figure 3.17: Distribution of $m^2_{1^{-+}} - m^2_{1^{++}}$ values from $\Pi^{(1)}$

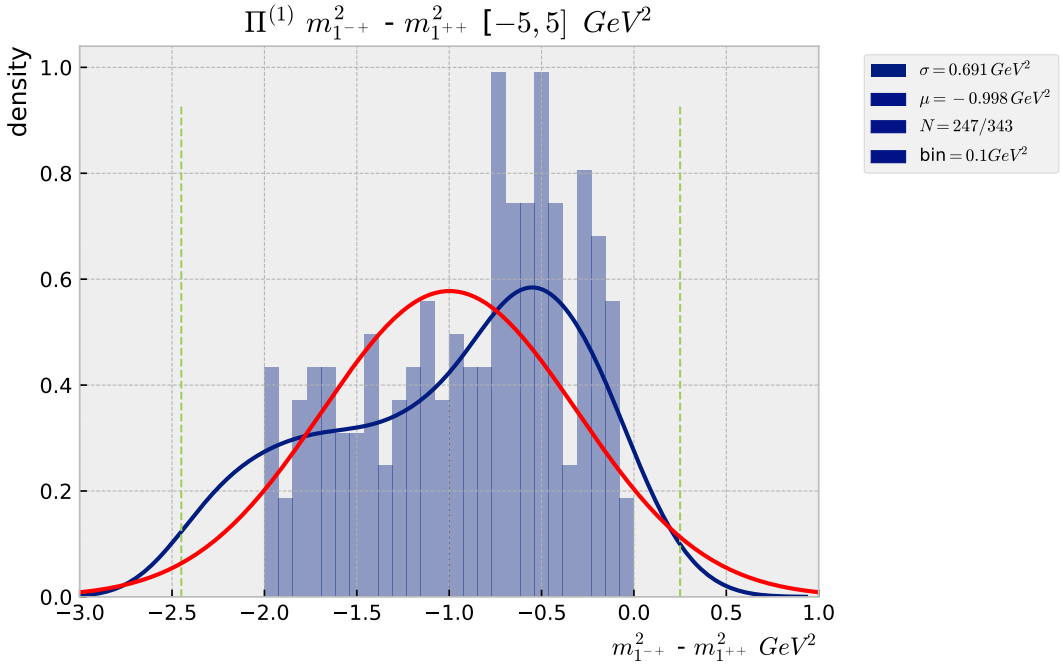

Figure 3.18: Highest peak distribution of $m^2_{1^{-+}} - m^2_{1^{++}}$ values from $\Pi^{(1)}$

In the last comparison in Figure 3.17, the mass squared values which show a skewing towards the lower end are obtained from the same correlation function $\Pi^{(1)}$, the mean value is considerably small which is $-0.0245\ GeV^2$ and may indicate that the masses of these partners are again expected in the same small range. With the standard deviation $2.19\ GeV^2$ and sample size of 343, again more descriptive information on the mass of 1^{-+} can be said whilst examining the sets and the behaviour of the Borel transformed correlation functions and their corresponding derivatives.

The highest peak of Figure 3.17 is shown in the Figure 3.18. The distribution resembles a beta function probability distribution. Again including most of the data from the full range of the splitting, the distribution shows the mean value $-0.998\ GeV^2$ with the standard deviation of $0.691\ GeV^2$. This might indicate an expectation of lower mass value for the 1^{-+} partner. Nevertheless, the small number of data can be improved in order to reach more precise results.

CHAPTER 4

CONCLUSION

The analyses performed yielded squared mass values of the J^{PC} partners of the $X(3872)$ particle as given in the figures in Chapter 3. With the obtained results, summarised in Table 4.1.

Correlation Function	$\Delta m^2_{J^{PC}}$	Total Distribution (GeV^2)	Highest Peak Distribution (GeV^2)	HQSS Expectation [73, 74](GeV^2)
$\Pi^{(2)}$	$m^2_{2^{++}} - m^2_{1^{++}}$	0.0375 ± 2.02	0.235 ± 0.807	$1.11^{\dagger}_{-0.00}$
$\Pi^{(2)}$	$m^2_{0^{++}} - m^2_{1^{++}}$	1.31 ± 1.95	1.77 ± 0.926	$-0.55^{+1.05}_{-0.69}$
$\Pi^{(1)}$	$m^2_{1^{-+}} - m^2_{1^{++}}$	-0.0245 ± 2.19	-0.998 ± 0.691	$0.11^{+0.56}_{-0.55}$

Table 4.1: Summary of squared mass comparison results. †: Upper bound is not set precisely.

As stated in Chapter 1, heavy quark spin symmetry suggests the presence of partners for the particles involving heavy quarks. In the current proposed here, there is charmonium contribution that results in the degeneracy of the states which are represented here as 2^{++}, 1^{++}, 1^{-+}, and 0^{++}. From these partners, 1^{++} partner is observed in the experiments [23] which is why the squared masses of particles are examined with comparison to the values of squared mass values of the 1^{++} partner. Theoretical values are obtained from [73] and [74] in order to compare the obtained results in this study with the previously conducted research.

In the results, one can observe the splitting between states 2^{++} and 1^{++} is almost uniform with a low mean value with some uniform like distribution at either end of the distribution. The mean value implies the splitting between these states at $J = 2$

follows more of a Gaussian distribution, hence the partner 2^{++} is expected in the same mass interval with the 1^{++} partner of $X(3872)$. Nonetheless, the values at uniform like tails might indicate the sets constructed of the variables might be incompatible with the correlation functions hence requiring a further investigation.

For the 0^{++} and 1^{++} couple, the distribution obtained suggests a higher mass value the 0^{++} partner which is expected around $1\ GeV^2$ higher in the degeneracy of $J = 2$ current. This also brings up the question of meson-meson interaction as well thus the structure cannot be concluded as tetraquark precisely [69]. This however still needs to be further examined with the sets of values and corresponding Borel transformed correlation functions and their derivatives as the standard deviation is found rather large. The results of these comparisons might be improved with the increase of the sample size as well.

Figures 3.17 and 3.18 show again very small mean values from these, one may deduce that the degeneracy of $J = 1$ states shows a more uniform distribution compared to the previous pair of partners hence 1^{-+} partner of $X(3872)$ is also expected to have the same mass as the 1^{++} partner in the $J = 1$ current.

In all splittings, one can compare the obtained results to the previous studies [73, 74] along with the experimental result on the partner 1^{++} [75] as given in the last column on Table 4.1. In the first splitting which is 2^{++} and 1^{++}, the values found in the previous studies [73, 74] match with the findings obtained here and the mass of 2^{++} can be expected in the same mass range with 1^{++}.

In the splitting of 0^{++} and 1^{++}, the distribution of the highest peak follows more of a uniform trend while including the splitting value obtained from the theoretical result in [73, 74] and the experimental result [75] which can be considered viable. In addition, since both results indicate a higher mass value for 0^{++} partner, the value of $m^2_{0^{++}}$ can be expected about $1\ GeV$ higher than $1m^2_{++}$. With the highest standard deviation in the results, the data should be examined further in order to reach a more definitive conclusion for this splitting.

The last pair of partners yielded a similar result with the first pair hence the results of $m^2_{1^{-+}}$ and $m^2_{1^{++}}$ can be interpreted as the masses of both partners are expected in

a similar range with no extreme splitting. Nevertheless, the generated sets should be examined further so as to interpret the results in a more precise manner.

In conclusion, when the results are examined and the current theories at hand are considered, it can be observed that the SVZSR method of the QCD shows that J^{PC} partners of the particle $X(3872)$ to have almost the same mass values for 2^{++} and 1^{++} from the current $j^2_{\mu\nu}$, and/or 1^{-+} partner to have the same mass with 1^{++} from the current $j^1_{\mu\nu}$. However, further study of these results and comparison with other proposed theoretical methods and further experimentation is necessary to proceed further to narrow the ranges of the predicted masses.

REFERENCES

[1] R. M. Albuquerque, J. M. Dias, K. Khemchandani, A. Martínez Torres, F. S. Navarra, M. Nielsen, and C. M. Zanetti, "QCD sum rules approach to the X, Y and Z states," *J. Phys. G*, vol. 46, no. 9, p. 093002, 2019.

[2] S. Choi *et al.*, "Observation of a narrow charmonium - like state in exclusive $B^{\pm} \to K^{\pm}\pi^{+}\pi^{-}J/\psi$ decays," *Phys. Rev. Lett.*, vol. 91, p. 262001, 2003.

[3] K. K. Seth, "An Alternative Interpretation of X(3872)," *Phys. Lett. B*, vol. 612, pp. 1–4, 2005.

[4] I. Adachi *et al.*, "Study of $X(3872)$ in B meson decays," in *34th International Conference on High Energy Physics*, 9 2008.

[5] B. Aubert *et al.*, "Study of the $B \to J/\psi K^{-}\pi^{+}\pi^{-}$ decay and measurement of the $B \to X(3872)K^{-}$ branching fraction," *Phys. Rev. D*, vol. 71, p. 071103, 2005.

[6] S.-K. Choi *et al.*, "Bounds on the width, mass difference and other properties of $X(3872) \to \pi^{+}\pi^{-}J/\psi$ decays," *Phys. Rev. D*, vol. 84, p. 052004, 2011.

[7] D. Acosta *et al.*, "Observation of the narrow state $X(3872) \to J/\psi\pi^{+}\pi^{-}$ in $\bar{p}p$ collisions at $\sqrt{s} = 1.96$ TeV," *Phys. Rev. Lett.*, vol. 93, p. 072001, 2004.

[8] T. Aaltonen *et al.*, "Precision Measurement of the $X(3872)$ Mass in $J/\psi\pi^{+}\pi^{-}$ Decays," *Phys. Rev. Lett.*, vol. 103, p. 152001, 2009.

[9] A. Abulencia *et al.*, "Analysis of the quantum numbers J^{PC} of the $X(3872)$," *Phys. Rev. Lett.*, vol. 98, p. 132002, 2007.

[10] B. Aubert *et al.*, "A Study of $B \to X(3872)K$, with $X(3872) \to J/\Psi\pi^{+}\pi^{-}$," *Phys. Rev. D*, vol. 77, p. 111101, 2008.

[11] V. Abazov *et al.*, "Observation and properties of the $X(3872)$ decaying to

$J/\psi\pi^+\pi^-$ in $p\bar{p}$ collisions at $\sqrt{s} = 1.96$ TeV," *Phys. Rev. Lett.*, vol. 93, p. 162002, 2004.

[12] K. Abe *et al.*, "Evidence for $X(3872) \to \gamma J/\psi$ and the sub-threshold decay $X(3872) \to \omega J/\psi$," in 22^{nd} *International Symposium on Lepton-Photon Interactions at High Energy (LP 2005)*, 5 2005.

[13] P. del Amo Sanchez *et al.*, "Evidence for the decay X(3872) —> J/ psi omega," *Phys. Rev. D*, vol. 82, p. 011101, 2010.

[14] G. Gokhroo *et al.*, "Observation of a Near-threshold D0 anti-D0 pi0 Enhancement in B —> D0 anti-D0 pi0 K Decay," *Phys. Rev. Lett.*, vol. 97, p. 162002, 2006.

[15] K. Abe *et al.*, "Experimental constraints on the possible J^{PC} quantum numbers of the $X(3872)$," in *22nd International Symposium on Lepton-Photon Interactions at High Energy (LP 2005)*, 2005.

[16] T. Aushev *et al.*, "Study of the $B \to X(3872)(D^{*0}\bar{D}^0)K$ decay," *Phys. Rev. D*, vol. 81, p. 031103, 2010.

[17] B. Aubert *et al.*, "Study of Resonances in Exclusive B Decays to anti-D(*) D(*) K," *Phys. Rev. D*, vol. 77, p. 011102, 2008.

[18] B. Aubert *et al.*, "Search for $B^+ \to X(3872)K^+$, $X(3872) \to J/\psi\gamma$," *Phys. Rev. D*, vol. 74, p. 071101, 2006.

[19] B. Aubert *et al.*, "Evidence for $X(3872) \to \psi_{2S}\gamma$ in $B^\pm \to X(3872)K^\pm$ decays, and a study of $B \to c\bar{c}\gamma K$," *Phys. Rev. Lett.*, vol. 102, p. 132001, 2009.

[20] R. Aaij *et al.*, "Evidence for the decay $X(3872) \to \psi(2S)\gamma$," *Nucl. Phys. B*, vol. 886, pp. 665–680, 2014.

[21] M. Ablikim *et al.*, "Observation of $e^+\ e^- \to \gamma\ X(3872)$ at BESIII," *Phys. Rev. Lett.*, vol. 112, no. 9, p. 092001, 2014.

[22] R. Aaij *et al.*, "Observation of $X(3872)$ production in pp collisions at $\sqrt{s} = 7$ TeV," *Eur. Phys. J. C*, vol. 72, p. 1972, 2012.

[23] R. Aaij *et al.*, "Determination of the X(3872) meson quantum numbers," *Phys. Rev. Lett.*, vol. 110, p. 222001, 2013.

[24] P. Zyla *et al.*, "Review of Particle Physics," *PTEP*, vol. 2020, no. 8, pp. 312–324, 2020.

[25] M. Gell-Mann, "Symmetries of baryons and mesons," *Phys. Rev.*, vol. 125, pp. 1067–1084, 1962.

[26] Y. Ne'eman, "Derivation of strong interactions from a gauge invariance," *Nucl. Phys.*, vol. 26, pp. 222–229, 1961.

[27] W. Heisenberg, "On the structure of atomic nuclei," *Z. Phys*, vol. 77, no. 1, 1932.

[28] M. Gell-Mann, "A Schematic Model of Baryons and Mesons," *Phys. Lett.*, vol. 8, pp. 214–215, 1964.

[29] G. Zweig, "An SU_3 model for strong interaction symmetry and its breaking; Version 2," Tech. Rep. CERN-TH-412, CERN, Feb 1964.

[30] M. Bander and J. D. Bjorken, "ASYMPTOTIC SUM RULES," *Phys. Rev.*, vol. 174, pp. 1704–1708, 1968.

[31] E. D. Bloom and F. J. Gilman, "Scaling, Duality, and the Behavior of Resonances in Inelastic electron-Proton Scattering," *Phys. Rev. Lett.*, vol. 25, p. 1140, 1970.

[32] H. Fritzsch, "The history of QCD," *CERN Courier*, vol. 52, pp. 21–25, Oct 2012.

[33] H. Fritzsch and M. Gell-Mann, "Current algebra: Quarks and what else?," in 16^{th} *International Conference on High-Energy Physics, ICHEP, Batavia, Illinois* (J. Jackson and A. Roberts, eds.), vol. C720906V2, pp. 135–165, 1972.

[34] E. de Rafael, "An Introduction to sum rules in QCD: Course," in *Les Houches Summer School in Theoretical Physics, Session 68: Probing the Standard Model of Particle Interactions*, 7 1997.

[35] M. A. Shifman, A. Vainshtein, and V. I. Zakharov, "QCD and Resonance Physics. Theoretical Foundations," *Nucl. Phys. B*, vol. 147, pp. 385–447, 1979.

[36] M. A. Shifman, A. I. Vainshtein, and V. I. Zakharov, "QCD and Resonance Physics: Applications," *Nucl. Phys. B*, vol. 147, pp. 448–518, 1979.

[37] R. M. Albuquerque, S. Narison, F. Fanomezana, A. Rabemananjara, D. Rabetiarivony, and G. Randriamanatrika, "Heavy-Light Exotics from QCD Laplace Sum Rules at N2LO in the chiral limit," *Nucl. Part. Phys. Proc.*, vol. 282-284, pp. 83–91, 2017.

[38] S. H. Lee, K. Morita, and M. Nielsen, "Width of exotics from QCD sum rules: Tetraquarks or molecules?," *Phys. Rev. D*, vol. 78, p. 076001, 2008.

[39] P. Colangelo and A. Khodjamirian, "QCD sum rules, a modern perspective," *At the frontier of particle physics*, pp. 1495–1576, 10 2000.

[40] D. B. Leinweber, "QCD Sum Rules for Skeptics," *Annals Phys.*, vol. 254, pp. 328–396, 1997.

[41] L. Maiani, F. Piccinini, A. D. Polosa, and V. Riquer, "Diquark-antidiquark states with hidden or open charm and the nature of $X(3872)$," *Phys. Rev. D*, vol. 71, p. 014028, Jan 2005.

[42] B. A. Li, "Is $X(3872)$ a possible candidate of hybrid meson," *Phys. Lett. B*, vol. 605, pp. 306–310, 2005.

[43] T. Barnes and S. Godfrey, "Charmonium options for the $X(3872)$," *Phys. Rev. D*, vol. 69, p. 054008, 2004.

[44] F. E. Close and P. R. Page, "The $D^{*0}\bar{D}^0$ threshold resonance," *Phys. Lett. B*, vol. 578, pp. 119–123, 2004.

[45] S. Pakvasa and M. Suzuki, "On the hidden charm state at 3872-MeV," *Phys. Lett. B*, vol. 579, pp. 67–73, 2004.

[46] M. Voloshin, "Interference and binding effects in decays of possible molecular component of $X(3872)$," *Phys. Lett. B*, vol. 579, pp. 316–320, 2004.

[47] C. Yuan, X. Mo, and P. Wang, "The Upper limit of the e+ e- partial width of $X(3872)$," *Phys. Lett. B*, vol. 579, pp. 74–78, 2004.

[48] C.-Y. Wong, "Molecular states of heavy quark mesons," *Phys. Rev. C*, vol. 69, p. 055202, 2004.

[49] E. Braaten and M. Kusunoki, "Low-energy universality and the new charmonium resonance at 3870-MeV," *Phys. Rev. D*, vol. 69, p. 074005, 2004.

[50] E. S. Swanson, "Short range structure in the $X(3872)$," *Phys. Lett. B*, vol. 588, pp. 189–195, 2004.

[51] T. Skwarnicki, "Heavy quarkonium," *Int. J. Mod. Phys. A*, vol. 19, pp. 1030–1045, 2004.

[52] E. J. Eichten, K. Lane, and C. Quigg, "Charmonium levels near threshold and the narrow state $X(3872) \rightarrow \pi^+\pi^- J/\psi$," *Phys. Rev. D*, vol. 69, p. 094019, 2004.

[53] L. Maiani, F. Piccinini, A. Polosa, and V. Riquer, "Diquark-antidiquarks with hidden or open charm and the nature of X(3872)," *Phys. Rev. D*, vol. 71, p. 014028, 2005.

[54] M. Takizawa and S. Takeuchi, "X(3872): A charmonium-molecule hybrid with isospin symmetry breaking," in *Workshop on Hadron and Nuclear Physics*, pp. 12–18, 2010.

[55] R. D. Matheus, S. Narison, M. Nielsen, and J. Richard, "Can the X(3872) be a 1^{++} four-quark state?," *Phys. Rev. D*, vol. 75, p. 014005, 2007.

[56] K. Terasaki, "A New Tetra-Quark Interpretation of $X(3872)$," *Progress of Theoretical Physics*, vol. 118, no. 4, p. 821–826, 2007.

[57] K. Terasaki, "Tetra-Quark Interpretation of X(3872) and Z_c(3900) Revisited," *arXiv High Energy Physics - Phenomenology (hep-ph)*, 2016.

[58] M. Neubert, "Heavy-quark symmetry," *Physics Reports*, vol. 245, no. 5, pp. 259–395, 1994.

[59] K. Abe *et al.*, "Experimental constraints on the possible J^{PC} quantum numbers of the $X(3872)$," in *22nd International Symposium on Lepton-Photon Interactions at High Energy (LP 2005)*, 5 2005.

[60] A. Abulencia *et al.*, "Measurement of the dipion mass spectrum in $X(3872) \to J/\psi\pi^+\pi^-$ decays.," *Phys. Rev. Lett.*, vol. 96, p. 102002, 2006.

[61] R. Aaij *et al.*, "Determination of the X(3872) meson quantum numbers," *Phys. Rev. Lett.*, vol. 110, p. 222001, 2013.

[62] K. Azizi and N. Er, "X(3872): propagating in a dense medium," *Nuclear Physics B*, vol. 936, pp. 151–168, 2018.

[63] M. Nielsen, F. S. Navarra, and S. H. Lee, "New Charmonium States in QCD Sum Rules: A Concise Review," *Phys. Rept.*, vol. 497, pp. 41–83, 2010.

[64] H.-W. Ke, X. Han, X.-H. Liu, and Y.-L. Shi, "Tetraquark state $X(6900)$ and the interaction between diquark and antidiquark," *Eur. Phys. J. C*, vol. 81, no. 5, p. 427, 2021.

[65] J. M. Dias, X. Liu, and M. Nielsen, "Predicition for the decay width of a charged state near the $D_s\bar{D}^*/D_s^*\bar{D}$ threshold," *Phys. Rev. D*, vol. 88, no. 9, p. 096014, 2013.

[66] J. M. Dias, F. S. Navarra, M. Nielsen, and C. M. Zanetti, "$Z_c^+(3900)$ decay width in QCD sum rules," *Phys. Rev. D*, vol. 88, no. 1, p. 016004, 2013.

[67] J. M. Dias, K. P. Khemchandani, A. Martínez Torres, M. Nielsen, and C. M. Zanetti, "A QCD sum rule calculation of the $X^{\pm}(5568) \to B_s^0\pi^{\pm}$ decay width," *Phys. Lett. B*, vol. 758, pp. 235–238, 2016.

[68] F. O. Duraes, S. H. Lee, F. S. Navarra, and M. Nielsen, "J / psi dissociation by pions in QCD," *Phys. Lett. B*, vol. 564, pp. 97–103, 2003.

[69] R. N. Faustov, V. O. Galkin, and E. M. Savchenko, "Heavy tetraquarks in the relativistic quark model," *Universe*, vol. 7, no. 4, p. 94, 2021.

[70] C. Hidalgo-Duque, J. Nieves, A. Ozpineci, and V. Zamiralov, "$X(3872)$ and its Partners in the Heavy Quark Limit of QCD," *Physics Letters B*, vol. 727, no. 4-5, p. 432–437, 2013.

[71] T. M. Aliev, K. Azizi, and A. Ozpineci, "Radiative Decays of the Heavy Flavored Baryons in Light Cone QCD Sum Rules," *Phys. Rev. D*, vol. 79, p. 056005, 2009.

[72] H. Mutuk, Y. Saraç, H. Gümüs, and A. Ozpineci, "X(3872) and Its Heavy Quark Spin Symmetry Partners in QCD Sum Rules," *Eur. Phys. J. C*, vol. 78, no. 11, p. 904, 2018.

[73] J. Nieves and M. P. Valderrama, "The Heavy Quark Spin Symmetry Partners of the X(3872)," *Phys. Rev. D*, vol. 86, p. 056004, 2012.

[74] C. Hidalgo-Duque, J. Nieves, and M. P. Valderrama, "Light flavor and heavy quark spin symmetry in heavy meson molecules," *Phys. Rev. D*, vol. 87, no. 7, p. 076006, 2013.

[75] P. A. "Zyla and others", "$x(3872)$," Tech. Rep. 083C01, Particle Data Group, 2020.

Appendix A

MATHEMATICAL EXPRESSIONS

A.1 Gamma Function Integral Identities

The identity necessary for the integral form of $1/(x^2)^n$ can be obtained from

$$\Gamma(n) = \int_0^\infty dt\, t^{n-1}\, e^{-t} \tag{A.1}$$

By applying a change of variable $t \to tx^2$ where x^2 is a constant defined in Euclidean configuration space, hence $x^2 > 0$, one can obtain

$$\frac{1}{(x^2)^n} = \frac{1}{\Gamma(n)} \int_0^\infty dt\; t^{n-1} e^{-t\,x^2}. \tag{A.2}$$

A.2 Heaviside Function Integral Representation

$$\theta(x) = \frac{1}{2\pi\, i} \int_{-\infty}^{\infty} dz \frac{e^{izx}}{z - i\epsilon} \tag{A.3}$$

A.3 Borel Transformation

Borel Transformation of a correlation function that is defined in the Euclidean configuration space of the momentum four-vector k^2 is defined as

$$\Pi(M^2) = \hat{B}\left[\Pi(k^2)\right] = \lim_{\substack{n\to\infty \\ k^2\to\infty \\ \frac{k^2}{n}\equiv M^2}} \frac{(k^2)^{n+1}}{n!}\left(-\frac{d}{dk^2}\right)^n \Pi(k^2) \tag{A.4}$$

Borel transforms of simple functions are given as below.

1. $\hat{B}\left[(k^2)^l\right] = 0$
2. $\hat{B}\left[\dfrac{1}{(k^2)^l}\right] = \dfrac{(-1)^l}{(l-1)!\,(M^2)^{l-1}}$
3. $\hat{B}\left[\dfrac{1}{(s+k^2)^l}\right] = \dfrac{e^{-s/M^2}}{(l-1)!\,(M^2)^{l-1}}$

A.4 Polarisation Operator Identities

Polarisation operators here are ϵ_μ and $\epsilon_{\mu\nu}$ that are of the vector and tensor particles corresponding to spin-1 and spin-2, respectively. For the vector particle, one has the identities

$$\begin{aligned} k^\mu \epsilon_\mu &= 0 \\ \epsilon_\mu \epsilon^{\mu *} &= -1 \\ k^\mu \epsilon_{\mu\nu} &= 0 \\ \epsilon_{\mu\nu} &= \epsilon_{\nu\mu} \\ \epsilon_{\mu\nu} g^{\mu\nu} &= 0 \\ \epsilon_{\mu\nu} \epsilon^{\mu\nu *} &= 1 \end{aligned} \tag{A.5}$$

with their spin sum

$$\sum_{\text{polarisation}} \epsilon_\mu \epsilon_\nu^* = -\left(g_{\mu\nu} - \frac{k_\mu k_\nu}{k^2}\right). \tag{A.6}$$

For the tensor particles,

$$\begin{aligned}\sum_{\text{polarisation}} \epsilon_{\mu\nu}\epsilon^*_{\alpha\beta} =& -\frac{1}{2}\left[\left(g_{\mu\alpha}-\frac{k_\mu k_\alpha}{k^2}\right)\left(g_{\nu\beta}-\frac{k_\nu k_\beta}{k^2}\right)+\left(g_{\nu\alpha}-\frac{k_\nu k_\alpha}{k^2}\right)\left(g_{\mu\beta}-\frac{k_\mu k_\beta}{k^2}\right)\right. \\ & \left.-\frac{2}{3}\left(g_{\mu\nu}-\frac{k_\mu k_\nu}{k^2}\right)\left(g_{\alpha\beta}-\frac{k_\alpha k_\beta}{k^2}\right)\right] \\ =& -\frac{1}{2}\left[g^\perp_{\mu\alpha}g^\perp_{\nu\beta}+g^\perp_{\nu\alpha}g^\perp_{\mu\beta}-\frac{2}{3}g^\perp_{\mu nu}g^\perp_{\alpha\beta}\right].\end{aligned} \tag{A.7}$$

Appendix B

LIST OF COEFFICIENTS

Equation (B.1)

$$\Pi^{(0)4.1} = \frac{5\,N_c^2\,m_Q^4}{4\pi^8}\,\hat{B}\,[\Pi_1]$$

$$\Pi^{(0)4.2} = \frac{N_c^2\,m_Q^4}{\pi^8}\,\hat{B}\,[\Pi_2]$$

$$\Pi^{(1)4.1} = \frac{3\,N_c^2\,m_Q^4}{4\pi^8}\,\hat{B}\,[\Pi_1]$$

$$\Pi^{(2)4.1} = \frac{N_c^2\,m_Q^4}{8\pi^8}\,\hat{B}\,[\Pi_2]$$

$$\Pi^{(2)3.1.1} = \frac{3\,N_c\,m_Q^4\,m_q\,\langle\bar{q}q\rangle}{64\pi^6}\,\hat{B}\,[\Pi_5]$$

$$\Pi^{(1)3.1.1} = \frac{9\,N_c\,m_Q^4\,m_q\,\langle\bar{q}q\rangle}{32\pi^6}\,\hat{B}\,[\Pi_6]$$

$$\Pi^{(1)3.1.2} = \frac{3\,N_c\,m_Q^4\,m_q\,\langle\bar{q}q\rangle}{16\pi^6}\,\hat{B}\,[\Pi_6]$$

$$\Pi^{(0)3.1.1} = \frac{33\,N_c\,m_Q^4\,m_q\,\langle\bar{q}q\rangle}{64\pi^6}\,\hat{B}\,[\Pi_6]$$

$$\Pi^{(0)3.1.2} = \frac{-N_c\,m_Q^4\,m_q\,\langle\bar{q}q\rangle}{8\pi^6}\,\hat{B}\,[\Pi_6]$$

$$\Pi^{(2)3.2.1} = \frac{11\,N_c\,m_Q^4\,m_q\,\langle\bar{q}q\rangle}{64\pi^6}\,\hat{B}\,[\Pi_6]$$

$$\Pi^{(2)3.2.2} = \frac{7\,N_c\,m_Q^4\,m_q\,\langle\bar{q}q\rangle}{64\pi^6}\,\hat{B}\,[\Pi_6]$$

$$\Pi^{(1)3.2.1} = \frac{33\,N_c\,m_Q^4\,m_q\,\langle\bar{q}q\rangle}{32\pi^6}\,\hat{B}\,[\Pi_6]$$

$$\Pi^{(1)3.2.2} = \frac{15\,N_c\,m_Q^4\,m_q\,\langle\bar{q}q\rangle}{32\pi^6}\,\hat{B}\,[\Pi_6]$$

$$\Pi^{(0)3.2.1} = \frac{99\,N_c\,m_Q^4\,m_q\,\langle\bar{q}q\rangle}{64\pi^6}\,\hat{B}\,[\Pi_6]$$

$$\Pi^{(0)3.2.2} = \frac{51\,N_c\,m_Q^4\,m_q\,\langle\bar{q}q\rangle}{64\pi^6}\,\hat{B}\,[\Pi_6]$$

In the Equation block on the previous page, the numbering system is constructed from Equation 2.30 where the last number separated by dots are to represent the order of the integrals from left to right. Integrals with order m_q^2 are not included due to the expansion at hand being until the order of m_q.

c_{i}	Value
c_1	$\dfrac{i\, m_Q^2\, \pi^2}{384}$
c_2	$\dfrac{i\, m_Q^4\, \pi^2}{7680}$
c_3	$\dfrac{-i\, m_Q^4\, \pi^2}{96}$
c_4	$\dfrac{-i\, m_Q^2\, \pi^2}{1536}$
c_5	$\dfrac{i\, m_Q^2\, \pi^2}{32}$
c_6	$\dfrac{i\, m_Q^4\, \pi^2}{384}$

Table B.1: Coefficients of Borel transformed integrals with their corresponding coefficients for their derivatives

Appendix C

LIST OF INTEGRAL IDENTITIES

$$
\begin{aligned}
n=0; \quad & \rho(s) = \int_0^s d\alpha (s-\alpha) \int_0^1 dx \int_0^1 dy \; f(x,y)\, \delta(\alpha - s(x,y)) \\
n=1; \quad & \rho(s) = \int_0^s d\alpha \int_0^1 dx \int_0^1 dy \; f(x,y)\, \delta(\alpha - s(x,y)) \\
n=2; \quad & \rho(s) = \int_0^1 dx \int_0^1 dy \; f(x,y)\, \delta(s - s(x,y)) \\
n=3; \quad & \rho(s) = \frac{d}{ds} \left[\int_0^1 dx \int_0^1 dy \; f(x,y)\, \delta(s - s(x,y)) \right]
\end{aligned}
\tag{C.1}
$$

are the spectral densities corresponding to the n values of powers of t on Equation 2.38.

Borel transformed correlation functions and the form of their derivatives are given below.

$$
\hat{B}\left[\Pi_{\mathrm{i}}\right] = i\, c_{\mathrm{i}} \int_0^{s_0} ds \int_0^1 dx \int_0^{1-x} dy \; s^2\, e^{s/M^2} \frac{f_{\mathrm{i}}(x,y)}{x^2} \delta\left(s - \frac{m_Q^2}{4x} + \frac{m_Q^2}{4y} \right) \tag{C.2}
$$

and

$$
\frac{\partial \hat{B}\left[\Pi_{\mathrm{i}}\right]}{\partial \left(1/M^2\right)} = i\, c_{\mathrm{i}} \int_0^{s_0} ds \int_0^1 dx \int_0^{1-x} dy \; s^3\, e^{s/M^2} \int_0^1 \frac{f_{\mathrm{i}}(x,y)}{x^2} \delta\left(s - \frac{m_Q^2}{4x} + \frac{m_Q^2}{4y} \right) \tag{C.3}
$$

with

$$
\begin{aligned}
f_{\mathrm{i}}(x,y) =& \frac{1}{y^2}\left[1-4x+6x^2-4x^3-x^4\right] \\
&+\frac{4}{y}\left[3x-3x^2-1+x^3\right] \\
&+\left[-12x+6x^2-4y+y^2+4xy+6\right]
\end{aligned}
\tag{C.4}
$$

where i $= 1, 2, 3, 4, 5$. The integrals corresponding to the values 3 and 4 are eliminated due to the exclusion of their order. For i $= 6$,

$$
\begin{aligned}
\hat{B}\left[\Pi_6\right] =& i\,c_6\left[e^{-s_0/M^2}-1\right]\int_0^1 dx\int_0^{1-x} dy\;\frac{f_6(x,y)}{x^3}\delta\left(s_0-\frac{m_Q^2}{4x}+\frac{m_Q^2}{4y}\right) \\
&-i\,c_6\int_0^{s_0} ds\int_0^1 dx\int_0^{1-x} dy\;e^{-s/M^2}\frac{1}{M^2}\frac{f_6(x,y)}{x^3}\,\delta\left(s-\frac{m_Q^2}{4x}+\frac{m_Q^2}{4y}\right)
\end{aligned}
\tag{C.5}
$$

and

$$
\begin{aligned}
\frac{\partial\hat{B}\left[\Pi_6\right]}{\partial\left(1/M^2\right)} =& i\,c_6\,s_0\,e^{-s_0/M^2}\left[\int_0^1 dx\int_0^{1-x} dy\;\frac{f_6(x,y)}{x^3}\,\delta\left(s-\frac{m_Q^2}{4x}+\frac{m_Q^2}{4y}\right)\right]_{s=0}^{s=s_0} \\
&-i\,c_6\int_0^{s_0} ds\int_0^1 dx\int_0^{1-x} dy\,e^{-s/M^2}\frac{f_6(x,y)}{x^3}\delta\left(s-\frac{m_Q^2}{4x}+\frac{m_Q^2}{4y}\right)
\end{aligned}
\tag{C.6}
$$

with

$$
\begin{aligned}
f_6(x,y) =& \frac{1}{y^3}\left[-1+3x-3x^2+x^3\right] \\
&+\frac{3}{y^2}\left[1-2x+x^2\right] \\
&+\frac{1}{y}\left[-3+3x+y\right]
\end{aligned}
\tag{C.7}
$$

and c_{i} values are given in Table B.1.